Design and analysis of a new type of aircraft wing leading edge against bird-impact

Yadav Bharosh Kumar
School of Aeronautics, Northwestern Polytechnical University, Shaanxi Province, Xi'an City, P.R. China
bharoshinfo@mail.nwpu.edu.cn

Abstract

The aim of this research is to provide a new structural design of wing leading edge which is more resistive to bird strike according to safety measures mentioned in Federal Aviation Regulations (FAR 25.571). Bird-strike against wing leading edge is simulated in PAM-CRASH while structure of wing leading edge is modeled in CATIA V5. Bird in shape of cylindrical with hemispherical ends having a weight of 1.8 Kg is impacted against wing leading edge at a velocity of 150 m/s. Five new models of leading edge are developed and simulated. Those are named as case 2 to case 6. A traditional design of wing leading edge named as case 1 is also simulated under same conditions for results comparison with new designs. Each case is simulated for two scenarios of bird strike. The first scenario is when bird exactly hits the leading edge. The second scenario is when bird hits a position 125 mm vertically upward from leading edge. Simulation results showed that traditional design is more prone damage in first scenario than second scenario. Case 2 to 4 proved good in both scenario but these cases are much safer in first scenario. Case 5 and 6 showed good resistance to bird strike in first scenario but received considerable damage in second scenario. By comparing results of all cases, it is found that case 2 to 4 are better design for wing leading edge than traditional one.

Keywords: Wing Leading Edge, Bird strike, Smooth Particle Hydrodynamics (SPH), CATIA V5, PAM-CRASH.

Introduction

Men have started sharing sky with birds after the invention of aircrafts. This mutual sharing is prone to accidents. Although there are various other elements like hails, debris etc. but today majority of incidents caused by foreign object damage (FOD) is to be reported as bird strike. Although the size of bird is very small as compared to aircraft but high speed of aircraft makes the bird strike event as a dangerous phenomenon. First record of bird strike was documented by Wright brothers, the inventors of aircraft. In 1912, bird strike claimed first human fatality when Cal Rogers crashed in to sea after hitting a gull and jamming aircraft flight controls. Since then such accidents are increasing due to in air traffic. These accidents have claimed many human lives along with monetary and material losses. From 1990 to2013, in a period of 24 years, at least 66 aircraft and 26 lives have been lost in civil aviation due to bird strikes. Statistical indicates that 73% of all collision occurs near the ground below 500 ft. and 94% under 2500 ft., making the take-off and landing phases especially critical to bird strike[1].

Front facing components of aircraft are exposed to bird strike. These include windshield, radome, wing leading edge, engines, forward fuselage, empennage, landing gear, propeller etc. Figure-1 shows vulnerability of aircraft components to bird strike according to data provided in Dolbeer[2]. Furthermore, 29% bird strikes for engine and 26% for wing cause damage making these areas of aircraft highly damaged due to bird strike. Due to

dangerous consequences of bird strike, aviation authorities like Federal Aviation Administration (FAA) demand all forward-facing components of aircraft to have a certain level of resistance against bird strike. Some Federal Aviation Regulations (FAR) relating bird strike are listed in Table-1[3].

Table-1: FAA bird strike requirements.

Component	FAR	Requirements
Windshield	25.775 (b)	Bird of 4 lb. at cruise speed of aircraft at sea level does not penetrate windshield.
	25.775 (c)	Minimize danger to pilots from flying windshield fragments.
General Structure	25.571	Successful completion of flight after hit by a 4-lb. bird at cruise speed of aircraft at sea level or 85% of cruise speed at 8000 feet, which is more critical.
Empennage	25.631	Successful completion of flight after hit by an 8-lb. bird at cruise speed of aircraft at sea level
Duplicate Pitot Tubes	25.1323 (j)	Bird does not damage both tubes
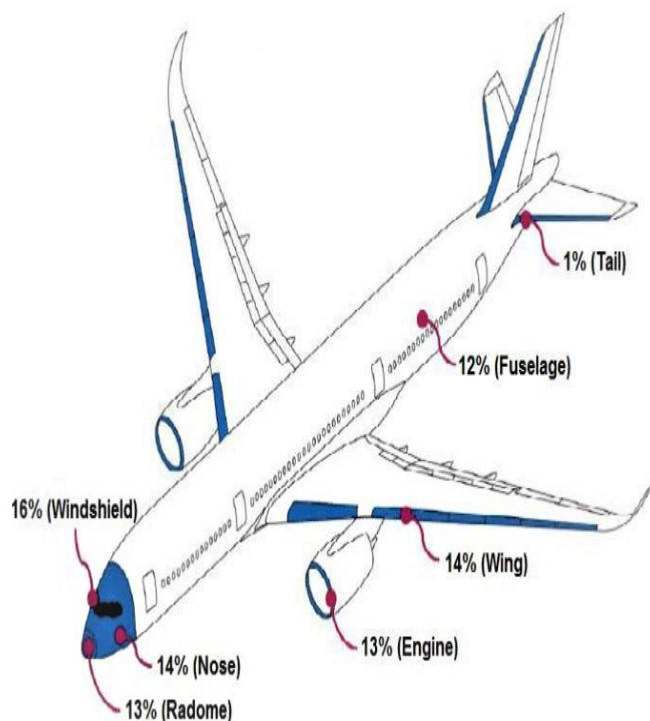
Figure-1: Vulnerability of aircraft-components to bird strike.

The subject of bird strike against aircraft is under discussion since the invention of aircraft and researchers are developing new techniques and design with growing aircraft industry. Computer invention has been accelerating more in this fields and some of the latest work performed in the field of bird strike are:

L. Jun[4] provided a tool for simulating the dynamic response of aircraft components against bird strike which can be used to assist designing bird strike resistive components. He conducted tests on sidewall of aircraft nose at a speed of 150 m/s and found that the behavior of a high-speed bird impact can be accurately simulated by the SPH method.

A. Grimaldi[5] found SPH approach to be most suitable and feasible methodology to simulate the dynamics of high speed phenomenon like bird strike against aircraft. Their study was focused on finite element analysis of an aircraft windshield-surround structure to satisfy the bird strike requirements according to European and US aviation regulations 25.631. A windshield model was subjected to an impact of a 1.8 kg bird model at a speed of 155 m/s with an impact angle of 90 degree. The results obtained during analysis showed that the energy transferred to the windshield during impact is strongly dependent of the impact angle.

It was also found that it is preferable to have a windshield structure with an impact angle smaller than 30 degree in order to design a structure capable to absorb safely the impact energy involved during the bird strike.

L. Jun[6] experimented bird impact at a flat plate at different striking velocities and simulated using an explicit finite element software PAM-CRASH with three bird material models. Comparison between experiment and simulation results suggested that smooth particle hydrodynamics (SPH) along with the Murnaghan equation of state for solid element is considered best for high velocity bird impact simulation.

Smojver[7] used modern numerical approach to predict the damage induced due to bird strike. They used coupled Eulerian Lagrangian (CEL) bird model in Abacus. This technique enabled them better capturing of fluid-like bird behavior upon impact in the velocity range at which bird strikes usually occurs.

U. A. Dar[8] performed finite element simulations to assess the dynamic response of windshield against high velocity bird impact. The bird with higher mass proved more fatal to the windshield as they impact more kinetic energy to the structure. Although the shape of the bird did not show significant effect in this study. These critical factors can be parameterized together to predict the combined effect on impact response of windshield and can provide certain guiding principles for windshield design and optimization.

K.V. Nikhil[9] used non-linear explicit finite element analysis to study bird strike phenomena. They used SPH method for modelling three types of birds, i.e. without void, bird with 20% void and bird with 40% void. The impact characteristics such as internal energy, kinetic energy, reaction force was computed by simulating collision of the different SPH bird models at 90 degree onto a flat rigid panel at an impact velocity of 50, 100 and 150 m/s. they found that presence of void inside the projectile plays a major role in the impact result.

The variation in velocity seems to affect the maximum reaction force and the internal, strain, kinetic energies significantly.

C.S. Stanley[10] used the experimental data of bird impact on a rigid flat plate to simulate different bird modelling techniques in FEM software ALTAIR RADIOSS. Aircraft wing leading edge was chosen to be simulated for bird impact at a velocity of 115 m/s. They found that Lagrangian technique approach for bird strike modeling resulted in large element distortion. Several options for time step controls were assessed; however, it altered the bird impact characteristics.

V.K. Goyal[11] found that SPH bird model is far more complex than the Lagrangian bird model and the number of variables influencing the SPH model is higher than for the Lagrangian one. Bird-strike events were divided into three separate problems: frontal impact on rigid flat plate, 0 and 30-degree impact on deformable tapered plate. Based on their results, they found that SPH method can be considered as a good alternative to simulate bird-strike events although it is more complex in the model creation.

V. Nagaraj[12] performed explicit finite element analysis to predict the bird strike induced impact damage on fuselage of a typical transport aircraft. A classical FE approach was adopted to model the fuselage of rectangular shape while Arbitrary Lagrangian - Eulerian (ALE) was used for modelling the bird. The ALE approach is still very good to simulate a real impact event, like the one on the fuselage, the results conducted in different metallic materials for AL2024-T4, AL7075-T6.

K. Nabil[13] used non-linear explicit code ANSYS AUTODYN to study the impact behavior of bird strike against wing leading edge structure. Two type of leading edge design were studied. Design A was comprised of skin, baffle, stiffener and two side ribs. Design B consisted of skin and four ribs. Aluminum was used for skin, stiffener and ribs while Kevlar epoxy composite for baffle. Simulated at different bird impact speeds, design B showed less deformation than design A and their results were close to experimental data.

P. Xue[14] studied bird strike against wing slat structure made of aluminum using elastic-plastic strain rate dependent model with damage in PAM-CRASH, commercial finite element dynamic software. Their simulation results showed that bird did not penetrated leading edge skin after impact and most of kinetic energy of bird, about 67%, was absorbed and consumed in large deformation of skin.

J.A. Reglero[15] analyzed the mechanical behavior of filled wing leading edge structures against hollow using standard bird impact tests. Results from bird strike tests on both type of structures showed that aluminum foam filled structure was 13% lighter in weight, four times better in global deformation behavior and two times better in load transmitting behavior than the hollow design.

Q. Sun[16] studied a new dynamic failure model using SPH method in LSDYNA on large aeroplane wing leading edge. It was found that impact location has an effect on impact damage.

R. Doubrava[17] tested various aircraft structures experimentally using air gun and simulated material properties, impector models and mesh characteristics using ABAQUS Explicit code. To simulate sharp parts like pitot probe or antenna, cylindrical shape was used for modelling bird. For oblique parts like wing leading edge and windshield, cylindrical with hemispherical ends shape was used for modeling bird.

R. Hedayati[18] studied bird impact using bird model similar to real bird and compared results with traditional bird models. The author suggested to choose ellipsoidal bird model for all bird impact simulations.

Kavitha Mol. S.[19] used ABAQUS/Explicit to study the parametric study of wing and empennage leading edges against bird strike. Three hundred simulations were performed to study the influence the effects of different parameters. It was found that leading edges deformation was dependent on parameters like elastic modulus, yield stress, hardening stress and hardening exponent. Poisson ratio of materials did not play much role in the deformation of structure.

L. Jun[20] impacted bird on aluminum 7075 plate and studied dynamic response of plate to be used in numerical simulation. High speed data acquisition equipment was used to measure strain values. The strain results obtained from simulation were compared with those from test results and fair agreement between the two was found.

The main objective of this research is to develop new structural designs of wing leading edge which are more capable of resisting a bird strike than a traditional design. The focus of these designs will be according to FAR 25.571 certification criteria. According to criteria, there should be no critical damage to front spar or wing box and successful completion of flight even if the bird penetrates leading edge skin. This must be proved for a bird weight of 1.8 kg striking the wing leading edge at operational speed[21].

In this research, to minimize damage to front spar will be the main theme of all designs. Weight of wing leading edge will be main design constraint in the study. Therefore, weight of new designs should not exceed than the traditional leading edge design.

Smooth Particle Hydrodynamics (SPH) Bird Modeling

In contrast to Lagrangian and Eulerian modeling techniques those use a regular finite element mesh, different meshless particles techniques were developed to achieve the objectives of independence from mesh distortion problem and computational efficiency. Smooth particle hydrodynamics (SPH) is one of these meshless modeling techniques.

Originally SPH technique was being used in simulation of astrophysical phenomenon like hypervelocity impacts where material shatters upon impact. During the decade of 1990, the technique was introduced to other fields to solve problems like continuum mechanics, crash simulation, ductile and brittle fracture of solids.

In SPH, fluid is represented by a set of discrete interacting particles independent of each other, capable of covering large deformations. Each particle is defined by a mass, velocity and material law, which is not localized but smoothed in space by an interpolation formula.

This interpolation formula is called kernel function. Field variables of an individual particle are calculated by interpolating its neighboring particles. A particle is considered in neighborhood when it is present in smoothing length of another particle. Comparison among different bird modelling techniques is summarized in Table-2[21].

Table-2: Comparison of bird modeling techniques.

Advantages	Disadvantages
Lagrangian Method	
• Simple Model Generation • Less solution time (before start of mesh distortion) • Impactor boundary well and clearly defined	• Severe deformation results in reduced time step, inaccuracy, artificial stiffening and error termination • Hour glass problems • Element erosion may cause reduction in mass
Eulerian Method	
• No mesh distortion • Constant time step • Large deformation handled • Stable simulations • Allow mixing of different materials within elements	• Complex model generation and result visualization • No clear outer boundary • Numerical leakage as total energy decreases with time • High computational cost • Fine mesh required in impact zone making process expensive
ALE Method	
• Interfaces and boundaries clearly defined • Good information of time history	• Thin section requires small time steps • Mesh motion constraint specification is needed
SPH Method	
• No mesh distortion • Constant time step • Numerically stable simulations • Capable of simulating complex bird splitting • Less computational time than Eulerian technique	• Complex model generation • No tensile behavior • Outer boundary is unclear • Higher computational time than Lagrangian Technique (before distortion of Lagrangian mesh)

Water is the major part of a real bird body. So, in bird impact analysis, a water type hydrodynamic behavior can be assumed as a valid approximation for a basic model. Also, there are several cavities like lungs, bones and special air sacs present inside body parts of a bird. Therefore, combine effect of all these factors reduces the average density of a bird. A homogenous material having density about 900 to 950 kg/m^3 can be used for modeling bird[22]. Typically, porous gelatin with a void content of 10 to 15% is used as artificial bird in bird strike testing. Gelatin having density of water nearly behaves as a real bird and is being widely used in bird strike testing. A cylindrical shaped with hemispherical ends gelatin substitute bird is shown in Figure-2[23].
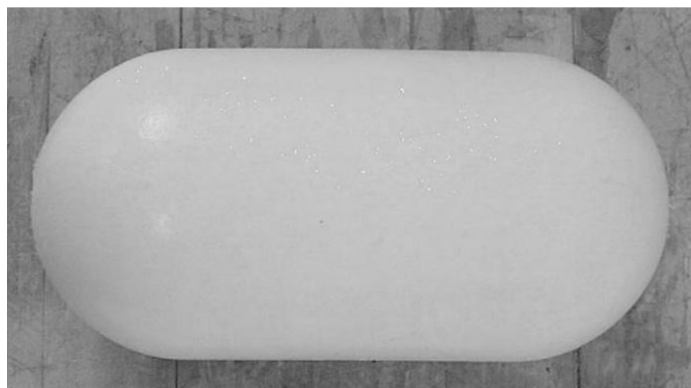
Figure-2: Gelatin artificial bird.

Bird Equation of State (EOS) Models: Equation of state (EOS) is much common method for modeling of bird impactor. EOS is a thermodymic relationship between volume (density), temperature (internal energy) and pressure[24]. This pressure P can be written as

$$P = P (V, T) = P (V, E) \qquad (2.5)$$

Where: V, T and E are volume, temperature and internal energy respectively. Johnson[25] used a polynomial form of EOS in which pressure p can be calculated as under.

$$p = C_0 + C_1\mu + C_2\mu^2 + C_3\mu^3 \qquad (2.6)$$

Where: C_0 , C_1 , C_2 and C_3 are constants depending on material and μ is a dimensionless quantity described as ratio of present density ρ to initial density ρ_0.

$$\mu = \frac{\rho}{\rho_0} - 1 \qquad (2.7)$$

Mc Carthy[26] used simpler Murnaghan EOS,

$$p = p_0 + B[\left(\frac{\rho}{\rho_0}\right)^\gamma - 1] \qquad (2.8)$$

Here, Here B and γ are material constants while ρ_0 is a reference pressure.

The Grüneisen EOS was adopted by Yupu[27] as written under,

$$p = \frac{p_0 c^2 \mu \left[1 + \left(1 - \frac{\gamma_0}{2}\right)\mu - \frac{a}{2}\mu^2\right]}{[1 - (S_1 - 1)\mu - S_2\frac{\mu^2}{\mu+1} - S_3\frac{\mu^3}{\mu+1}]^2} + (\gamma_0 + a\mu)E \qquad (2.9)$$

Here, γ_0 is the Grüneisen parameter, E is the internal energy and a, C, S_1, S_2 and S_3 are constants.

Structural and FE Modeling of Wing Leading Edge (WLE)

To design a new type of leading edge, wing of Airbus 320 is selected. A section of 2000 mm length from leading side is considered for study as shown in Figure-3. CATIA V5 is used to model the structural components of wing leading.
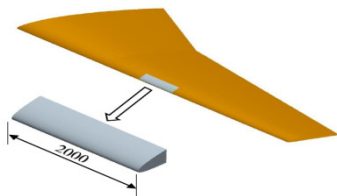
Figure-3: Leading edge of A320.

Six different structural design are designed for wing leading edge. First of these designs is conventional traditional design while remaining five are studied for better bird impact resistance relative to traditional design. All designs studied in this research are listed bellows: i. Case 1: Traditional Wing Leading Edge. ii. Case 2: Leading Edge with a Sub Spar, Heating Sheet and Angular Ribs. iii. Case 3: Leading Edge with Additional Skin for Front Ribs. iv. Case 4: Leading Edge with a Wedge Support and Straight Ribs. v. Case 5: Leading Edge with a Wedge Support having Inside Ribs. vi. Case 6: Leading Edge with a Wedge Support having Angular Front Ribs.

Case 1: Traditional Wing Leading Edge (WLE): The traditional design of wing leading consists of skin, front spar and ribs as shown in Figure-4. Skin thickness and front spar thicknesses are 2 mm and 5 mm respectively. Central four ribs have a wall thickness of 2 mm and 20 mm wide while two side ribs have a wall thickness of 2 mm and 30 mm wide. Ribs pitch distance is 372 mm. Skin is made of Al 2024 while front spar and ribs are made of Al 7075. The total weight of structure is 39.7 Kg.
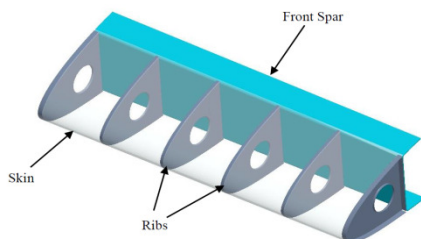

Figure-4: Case1: Traditional WLE Structure.

Case-2: Leading Edge with a Sub Spar, Heating Sheet and Angular Ribs: In this type of design, an extra sub spar and a heating sheet is added as shown in Figure-5 (Skin is being hidden). Sub spar is 1 mm thick and 40 mm wide while heating sheet is 5 mm thick. Sub spar is placed at a distance of 250 mm from the start of leading edge. Heating sheet is assembled to the skin with the help of a heating sheet support which is 2 mm thick. The skin in this case is 1 mm thick while front spar is similar to case 1. There are 18 ribs in total. Two of them are placed at the sides having wall thickness of 2 mm and 30 mm wide. Remaining 16 ribs are divided into 8 front ribs and 8 rear ribs separated by sub spar. All of these ribs have a wall thickness of 1 mm and 20 mm wide. Front ribs make at an angle of 91.5° between them while rear ribs makean angle of 96.5° towards the side of sub spar. Ribs pitch distance for both front and rear ribs is 485 mm. Skin material is Al 2024 while all other parts are made of Al 7075. The total weight of this structure is 39.3 Kg.
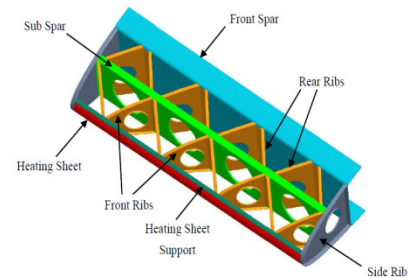

Figure-5: Case 2: Leading edge with a sub spar, heating sheet and angled ribs.

Case 3: Leading Edge with Additional Skin for Front Ribs

In case 3, as shown in Figure-6 (skin is being hidden), an additional skin is added to front portion of sub spar. This additional skin is 2 mm thick and covers front ribs only. There are 9 front ribs having a wall thickness of 1 mm and 20 mm wide. The front ribs pitch distance is 196 mm. Side ribs are like previously designs 1 mm thick and 30 mm wide. Sub Spar is moved forward and is now placed at 150 mm from starting edge of wing.
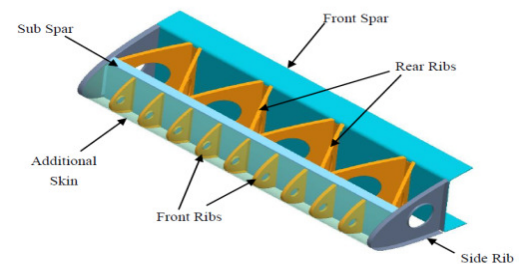

Figure-6: Case 3: Leading Edge with additional skin for front ribs.

Sub spar has a wall thickness of 1 mm and 40 mm wide. There are 8 rear ribs having wall thickness of 1 mm and are 20 mm wide. These ribs make an angle of 63° between them toward side of sub spar. The rear rib pitch distance is 485 mm. Front spar is 5 mm thick and 50 mm wide while skin is 1 mm thick. Skin material is Al 2024 while all other parts are made of Al 7075. Total weight of structure in this case is 38.5 kg.

Case-4: Leading Edge with a Wedge Support and Straight Front Ribs: The basic theme of this design is to cut the bird into two pieces with the help of a wedge support placed before sub spar. If wedge support successfully splits the bird into two pieces, then the bird will not impact the front spar directly. Instead it will pass from upper and lower side of front spar without harming it. The structural configuration of this design is shown in Figure-7 (skin is being hidden). The wedge support is 3 mm thick and its sides make an angle of 90.4° to flow of bird. There are 7 front ribs having a wall thickness of 1 mm and are 20 mm wide. The front rib pitch is 242.5 mm. The two side ribs are 30 mm wide and have a wall thickness of 1 mm. Sub spar is 63°. The rear ribpitch distance is 485 mm. Parameters of skin and front spar are same as in case 2. Material for skin is Al 2024 while Al 7075 is for all other parts. The weight of this structure is calculated as 39 kg.
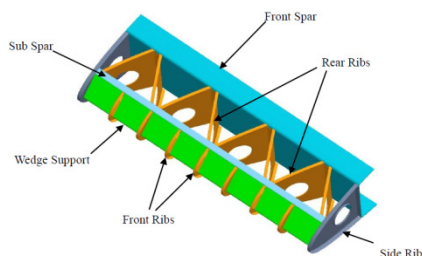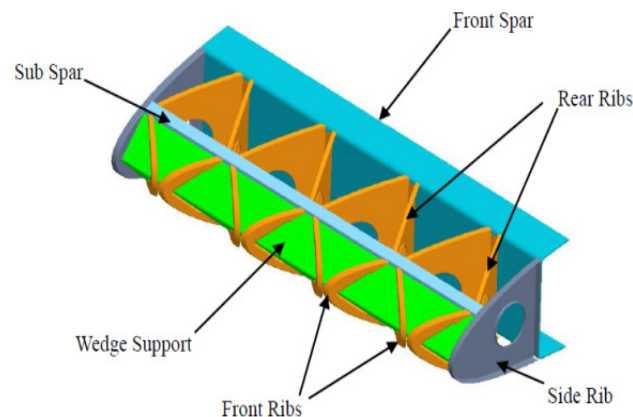

Figure-7: Case 4: Leading Edge with a wedge support and straight front ribs.

Case 5: Leading Edge with a Wedge Support Having Inside Front Ribs: In case 5 as shown in Figure-8, front wedge is supported by front ribs from inside. A wedge of 3 mm thickness is supported by 7 front ribs having wall thickness of 1 mm and are 20 mm wide. The front rib pitch distance is 242.5 mm. The remaining structure is similar to case 4. Total weight of structure in this case is 39.6 kg.
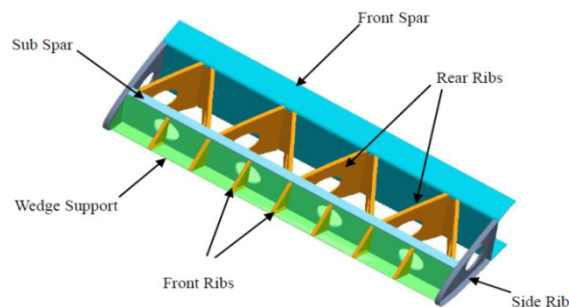
Figure-8: Case 5: Leading edge with a wedge support having inside front ribs.

Case 6: Leading Edge with a Wedge Support having Angular Front Ribs: In this case, wedge is supported by front angular ribs as shown in Figure-9. These front ribs are 20 mm wide and have 1 mm wall thickness. Ribs make angle of 105° towards leading edge start between them. Wedge and other remaining structure is similar to case 4. Total weight of leading edge for case 6 is also 39.6 kg.


Figure-9: Case 6: Leading edge with a wedge support Taper front ribs.

Explicit FE Analysis of Wing Leading Edge

It is very expensive to manufacture each design and test them against bird strike. To overcome this, several FE codes have been developed to simulate bird strike phenomena. In this research, commercially available FE software PAM-CRASH and Altair Hyper mesh are used for simulation. FE model of wing leading is modeled in PAM-CRASH while bird is modeled in Altair Hyper mesh. According to FAR 25.571, the weight of bird should be 4 lb. (1.81 kg) for which wing leading edge must be tested for bird strike and fulfill the requirements as mentioned in said rule.

The diameter of bird is 115 mm and length is 230 mm calculated for a density of 934 kg/m³. Thus, length to diameter ratio is maintained as 2 as preferred. The pitch distance for SPH particles is kept at 8 mm. Thus, the total number of SPH particles generated is 3705 and each particle containing a mass of 0.49 grams. SPH model of bird is shown in Figure-10. This SPH model of bird is imported into PAM-CRASH. Bird material in PAM-CRASH is defined by material 28 known as Murnaghan equation of state. The pressure for Murnaghan EOS is defined by equation (2.8).

Constant of Murnaghan EOS, B and γ cannot be measured directly[28] but their indirect measurement is possible. In current research, B = 9.3 GPa and γ = 7.14 are taken from[4]. This bird is given velocity of 150 m/s along the flying direction of aircraft according to criteria defined in FAR 25.571.
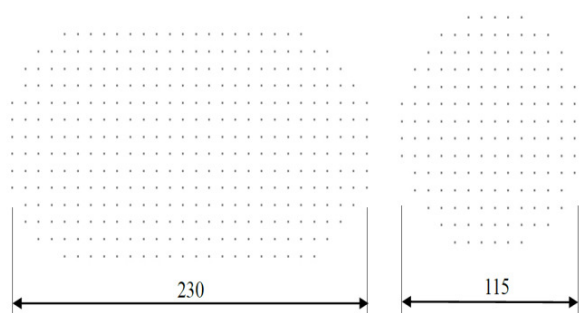
Figure-10: SPH model of birds.

In this study, shell element is used for FE analysis, PAM-CRASH provide a lot of shell elements for FE modeling and material type 102 is used. A meshed model of case 4 is shown in Figure-11. Skin and front spar are meshed using visual mesh using element size of 10 mm while ribs and sub spar are meshed using an element size 5mm, wedge support, heating sheet and heating support are meshed using an element size of 10 mm.

As described in previous, aluminum alloys Al 2024 and Al 7075 are being used as materials for components. Plastic response of these materials is defined by strain rate dependent Cowper-Symonds law. Cowper-Symonds law defines the yield strength of isotropic strain hardening of a strain rate dependent material[8]. The dynamic yield stress σ can be defined as:

$$\sigma = \left[a + b\left(\varepsilon_p\right)^n\right]\left[1 + \left(\tfrac{\dot{\varepsilon}}{D}\right)^{\frac{1}{\eta}}\right] \qquad (3.1)$$

Where: a = yield stress at zero plastic strain; b = Strain hardening co-efficient; ε_p = Plastic Strain; η = Strain hardening exponent; $\dot{\varepsilon}$ = Strain rate and D, η = Strain rate hardening co-efficient.

As these aluminum alloys[4], does not show much variation at different strain rates, so Al 2024 and Al 7075 can be considered insensitive for strain rate. Therefore, strain dependent term $\left[1 + \left(\tfrac{\dot{\varepsilon}}{D}\right)^{\frac{1}{\eta}}\right]$ in equation (3.1) can be ignored. The values Aluminum alloy of remaining parameters of equation (3.1) are listed in Table-3[4].

Analysis Setup: In this research, it is assumed that bird will hit the leading edge at a place between two ribs as this area is weaker to bird strike, as shown in Figure-12. The initial velocity of bird in each case is 150 m/s. This will be called first scenario. In second phase of analysis, bird will be shifted 125 mm vertically from its position in first scenario. Analysis will be performed for all cases like first scenario. This will be known as second scenario. The position of bird with respect to leading edge is shown in Figure-13.
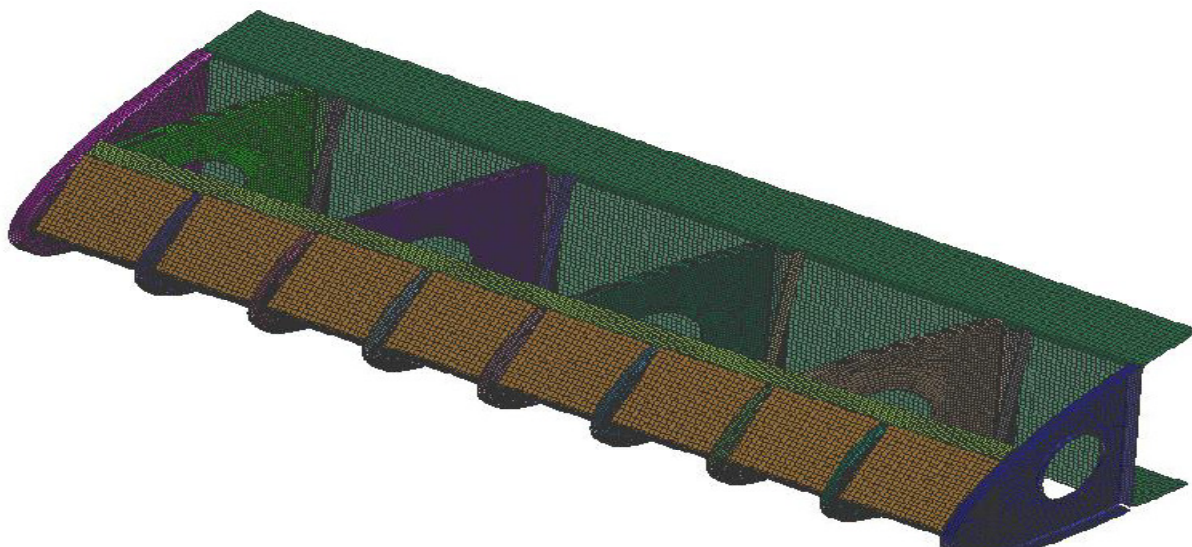
Figure-11: Meshed model for case 4.

Table-3: Material properties for aluminum alloy Al 2024 and Al 7075.

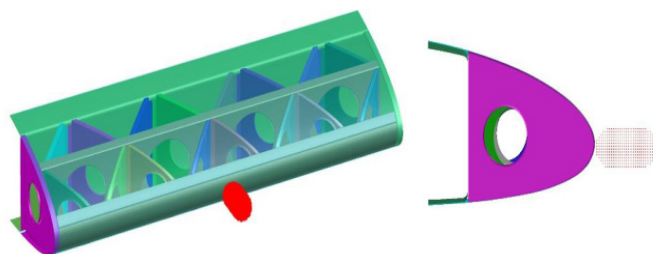| Material	a (MPa)	B(MPa)	η	Material	Density Kg/m³	Elastic Modulus GPa	Poisson Ratio	Failure Strain
Al 2024	350	426	0.34	Al 2024	2780	73	0.3	0.2
Al 7075	400	200	0.45	Al 7075	2810	71	0.3	0.14

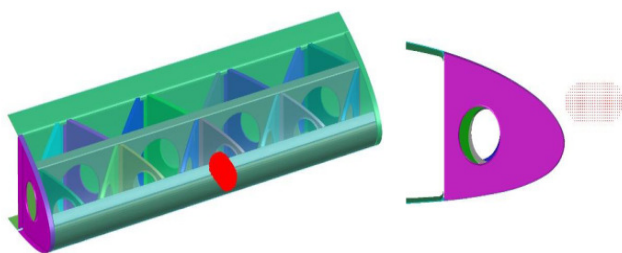**Figure-12:** 1ˢᵗ scenario bird strike setting.

Figure-13: 2ⁿᵈ scenario bird strike setting.

Results and discussion

Case-1: Traditional Wing Leading Edge: The impact process for this case is shown in Figure-13 with a time step of 2ms. Left hand side images show the condition of leading edge with skin while right side images show conditions of inner components by hiding skin.

Results shows that skin absorbed the maximum energy of impact. Skin internal energy is increased to 10.6 KJ from zero at the end of simulation which is almost half of the initial kinetic energy of bird. Bird has initially 20.3 KJ of kinetic energy before impact which is reduced to 1.4 KJ at the end of simulation. Rib present at the right side of impact zone takes 0.45 KJ while rib present at left side takes 0.4 KJ of energy.

The remaining ribs absorb an amount of energy ranging from 0.03 KJ to 0.02 KJ. Front spar has absorbed an energy of 0.88 KJ.

Since front spar is directly hit by the bird, therefore it got high stresses. The maximum stress in front spar is found to be 448 MPa at impact area, bypassing initial yield stress which is 400 MPa. It means that front spar has deformed plastically at impact area. The maximum plastic strain in front spar is found to be 0.037 which is 26% of failure strain listed in Table-3. The maximum deflection in the front spar is 26.4 mm. The time history of stress, strain and deflection for front spar is shown in Figure-14, Figure-15 and Figure-16.

Case-2: Leading Edge with a Sub Spar, Heating Sheet and Angular Ribs: Bird is hit at center of space present between front ribs and impact results are shown in Figure-17 at with a time interval of 2 ms after impact. Left side images present the impact details with skin while right side images show the damage of the leading edge inside components. The bird tries to

penetrate the thick heating sheet supported by heating sheet support resists bird penetration. Bird slips along skin and bypasses the remaining leading edge structure. The bird hit area of heating sheet, its support and two front ribs on each side of impact area are plastically deformed. Sub spar and rear ribs also deform plastically.

The bird hits the leading edge with kinetic energy of 20.3 KJ. In 10 ms, bird loses its 17.4 KJ of energy to wing leading parts. The major portion of bird energy is absorbed by skin whose internal energy is increased to 4.8 KJ from zero. Heating sheet and its support absorb 1.6 KJ and 1.9 KJ of bird impact energy respectively. Front ribs present at sides of impact zone takes 0.5 KJ and 0.6 KJ of bird energy. The newly introduced sub spar which is not present in case 1 absorbs only 0.07 KJ of energy. Rear ribs absorb a little amount of impact energy ranging from 0.04 KJ right behind impact line to 0.009 KJ present near side ribs. Each side rib takes 0.02 KJ of energy. Since most of energy is dissipated at front parts, only 0.06 KJ energy is absorbed by front spar.

As very little energy of impact manages to approach the front spar, therefore stress level in front spar remains much lower. Results show that there is no plastic strain produced in front spar. So, the material behavior of front spar is in elastic range. The maximum stress in front spar is found to be 209 MPa present at right corner of rear edge. The maximum displacement for front spar is found to be 1.7 mm at center of front left edge. The time history of stress and displacement for front spar is shown in Figure-18 and Figure-19.

Case 3: Leading Edge with Additional Skin for Front Ribs: Bird impact results at different time interval for case 3 are shown in Figure-21 with skin on left side images and with skin hidden on right side images. It is clear from images that bird does not penetrate wing leading edge even the skin. Bird hits the leading edge, produces a big dent and then splits away. The situation of front ribs is shown in Figure-20. From figure, it is clear that two ribs at the sides of impact area are almost destroyed.

Most of the impact energy is absorbed by skin and secondary additional skin. Skin takes an amount of 2.2 KJ while additional skin takes 6.9 KJ of energy. The two destroyed ribs absorb 0.38 KJ of energy each. Front spar absorbs only 0.04 KJ of energy. The bird kinetic energy is reduced to 4.3 KJ from initial value of 20.3 KJ after 10ms.

Like previous case, a little amount of impact energy is transferred to front spar. Results show that there is no plastic strain produced in front spar. Maximum stress in front spar is found to be 186 MPa which is present at the lower side of area mating with rear rib situated right behind impact line. Maximum deflection is 1.7 mm at same area where maximum stress occurs. Time history of stress and displacement in front spar is shown in Figure-22 and Figure-23.
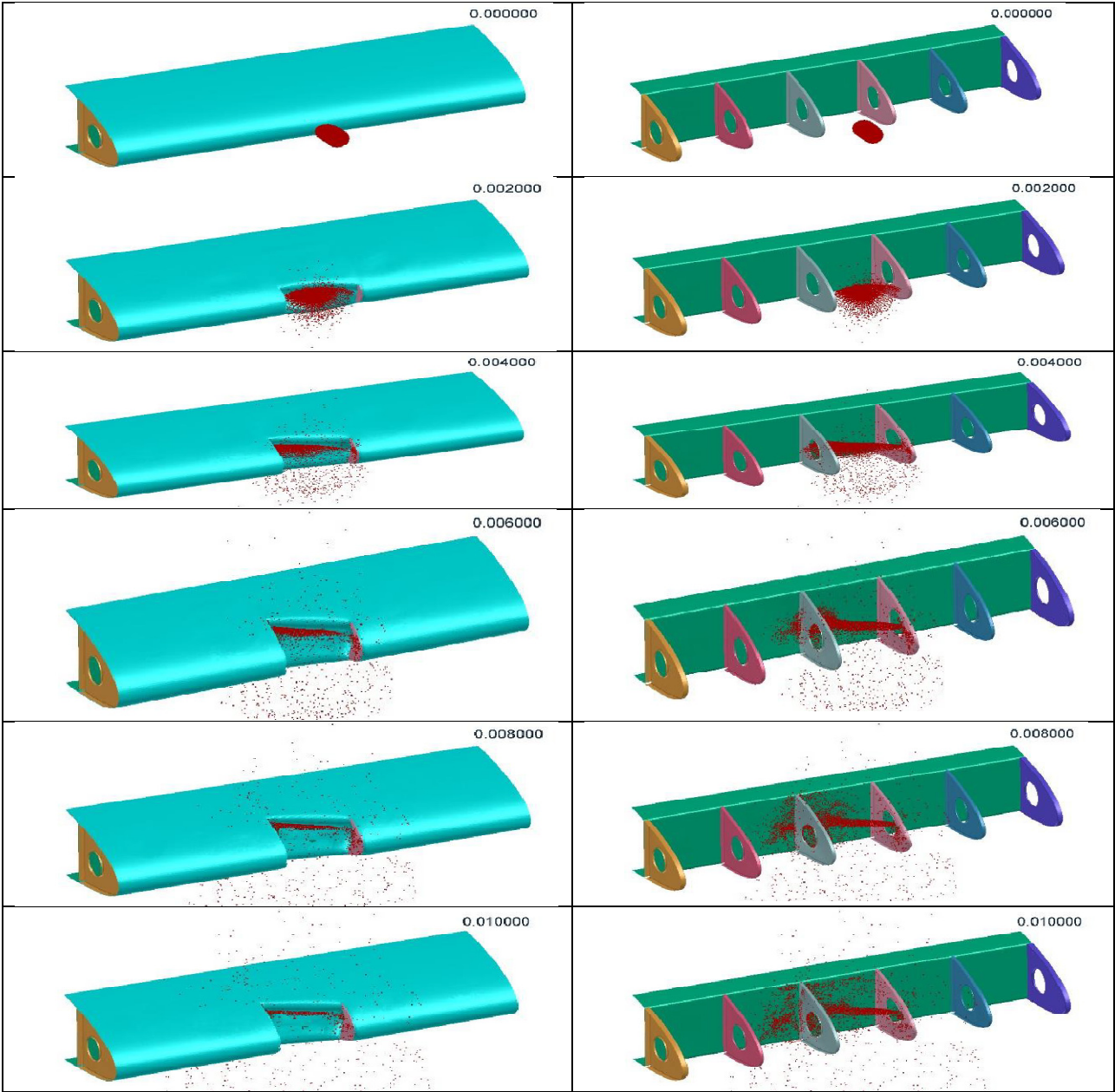
Figure-13: Case 1: Wing leading edge condition with a time interval of 2ms.
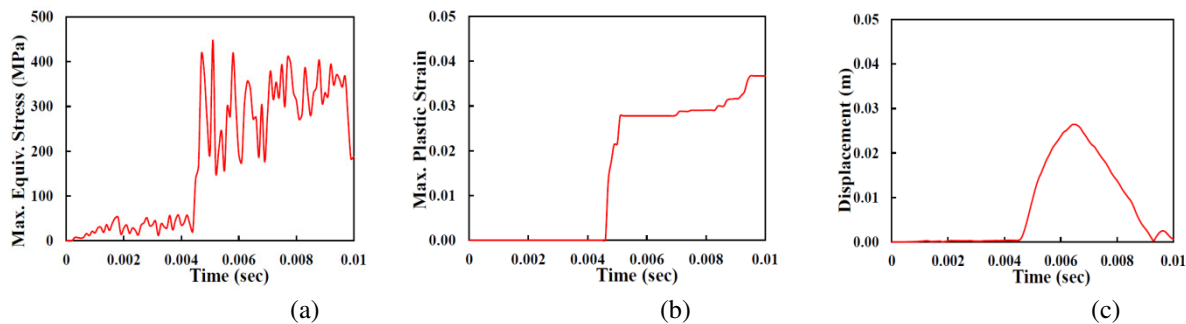

(a)   (b)   (c)

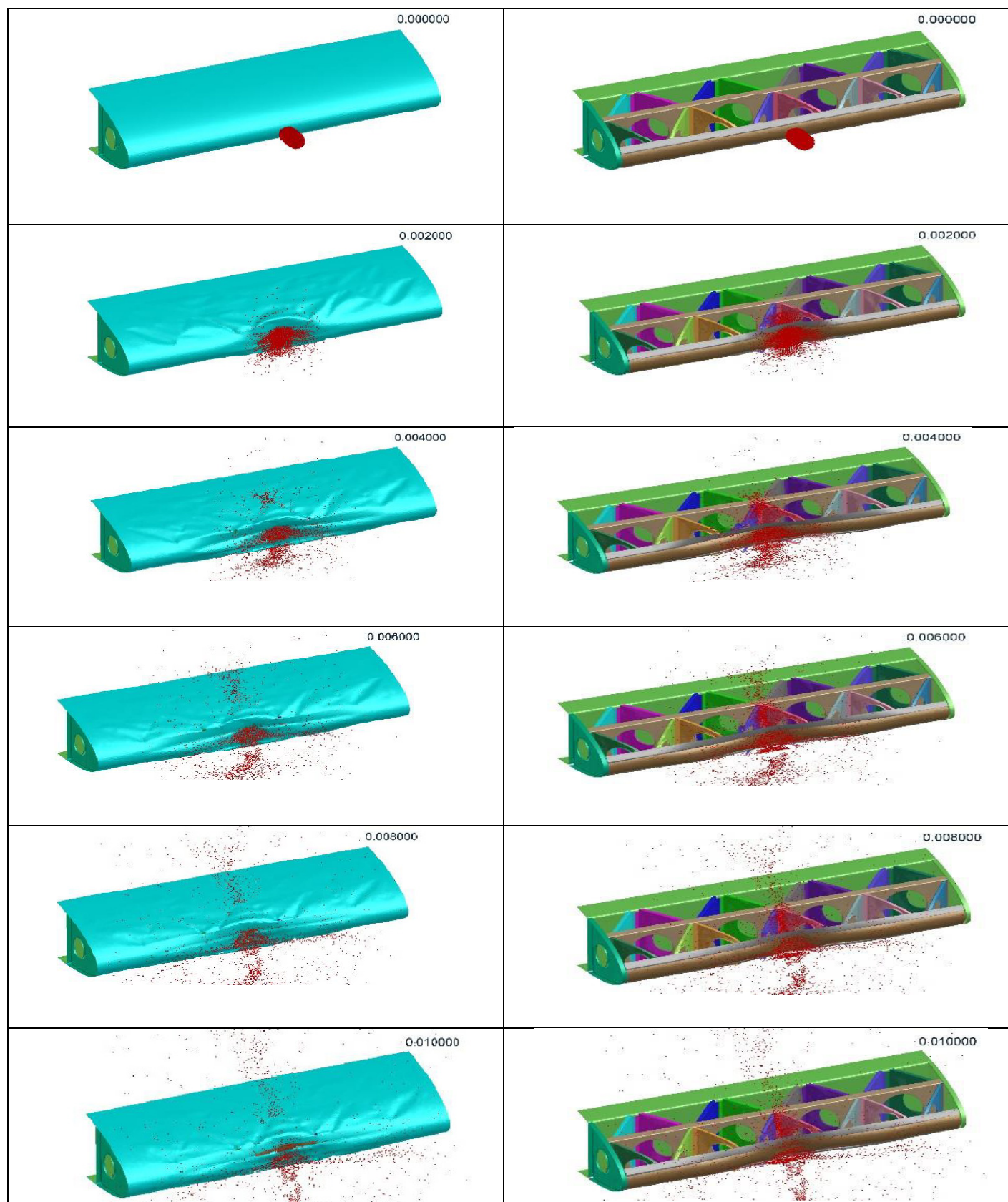**Figure-14, Figure-15, Figure-16:** Case 1 Stress, Plastic Strain and Displacement history for front spar.

Figure-17: Case 2: Wing leading edge condition with a time interval of 2ms.
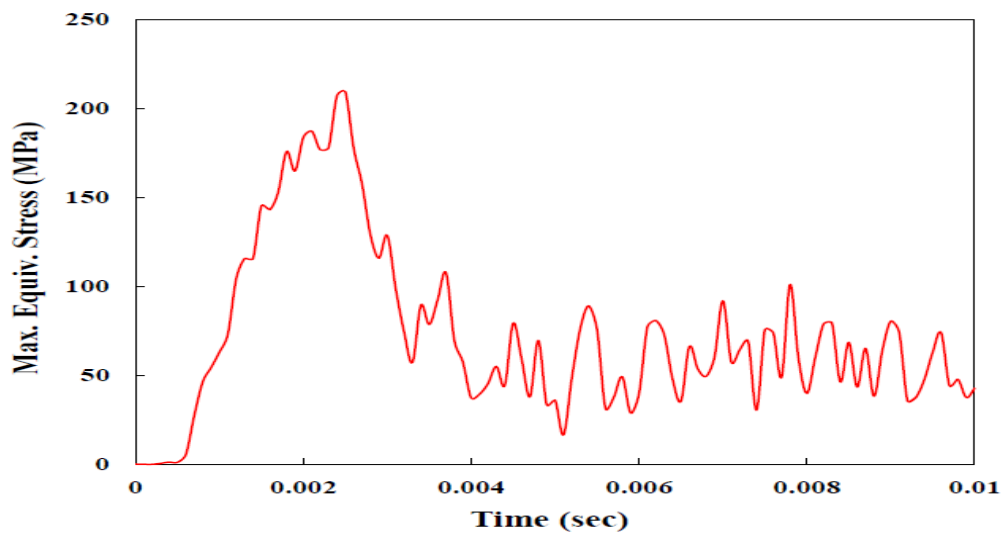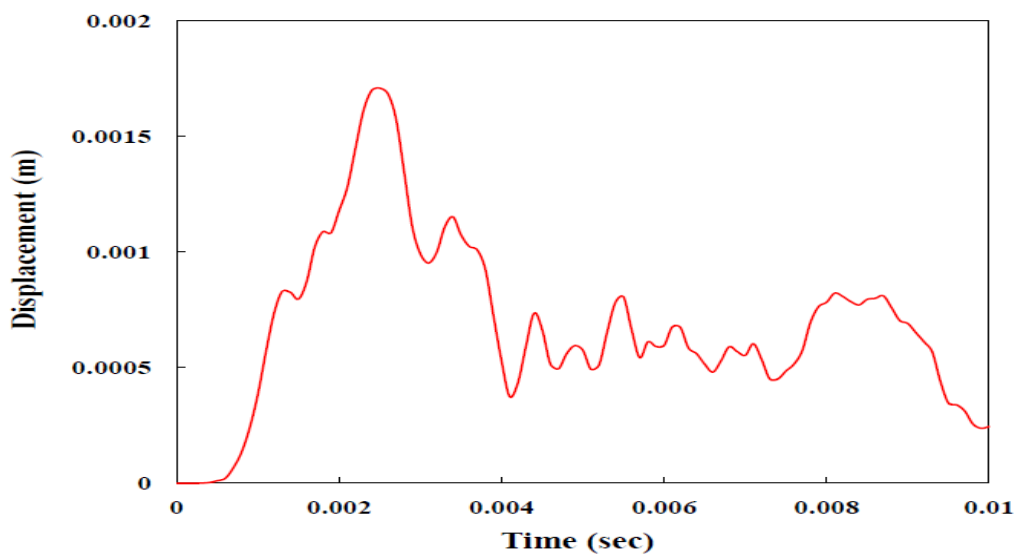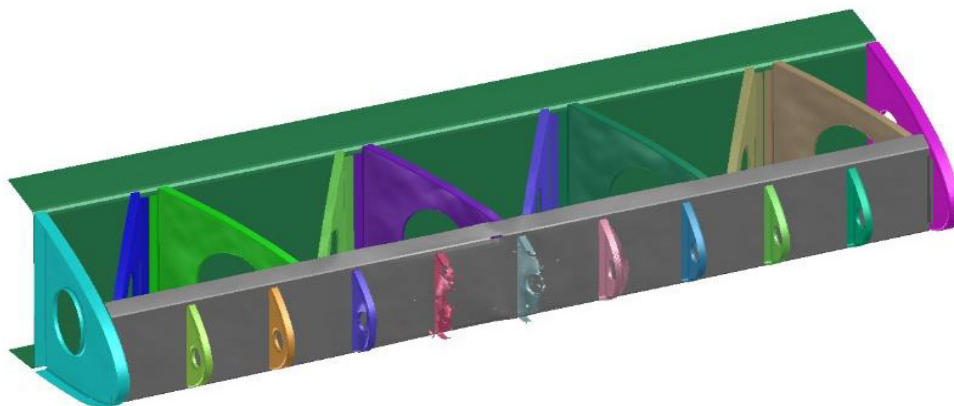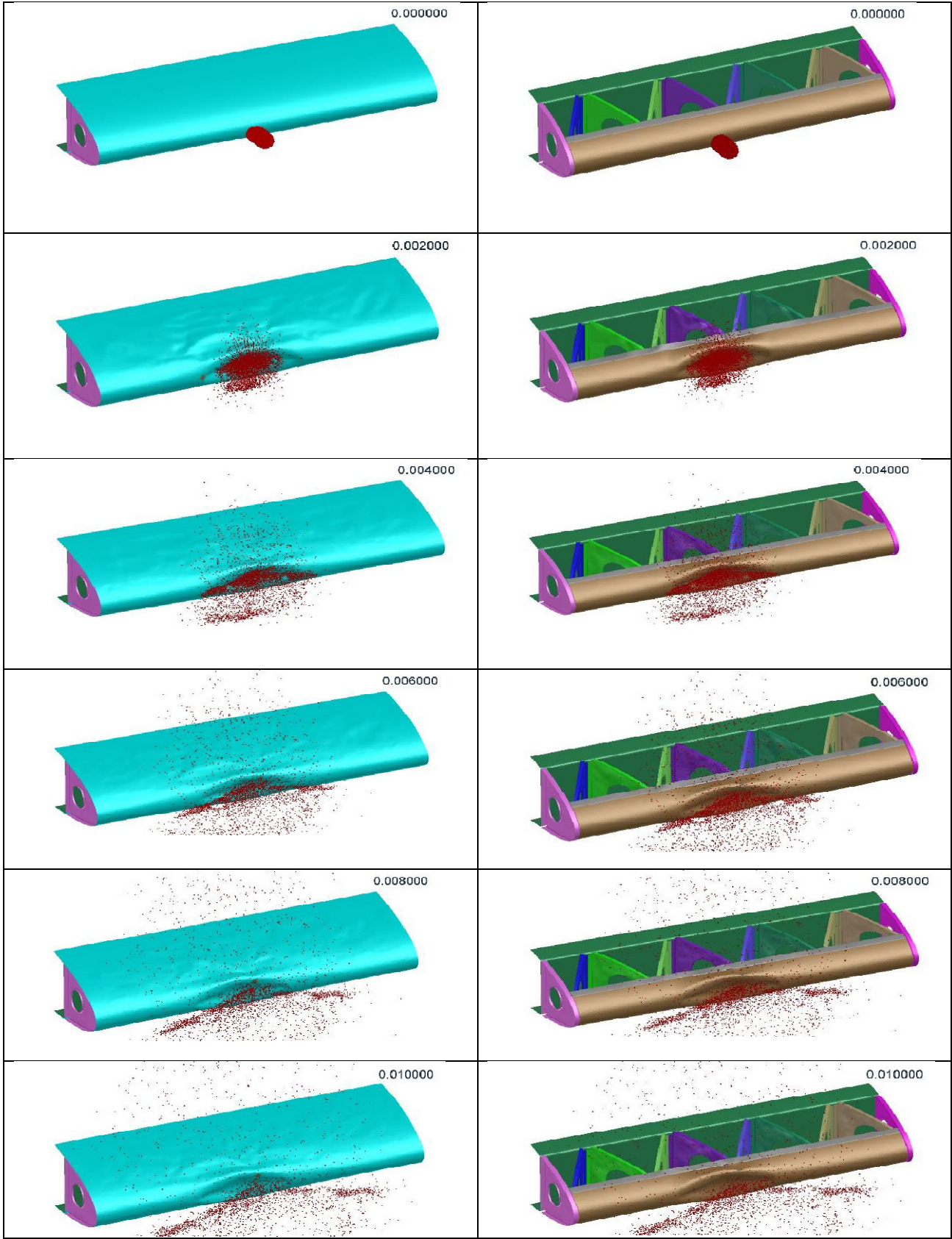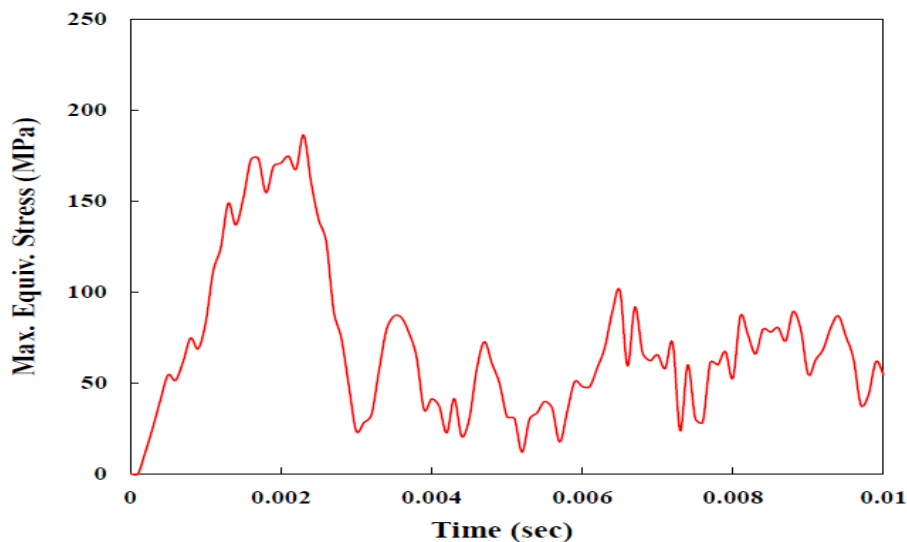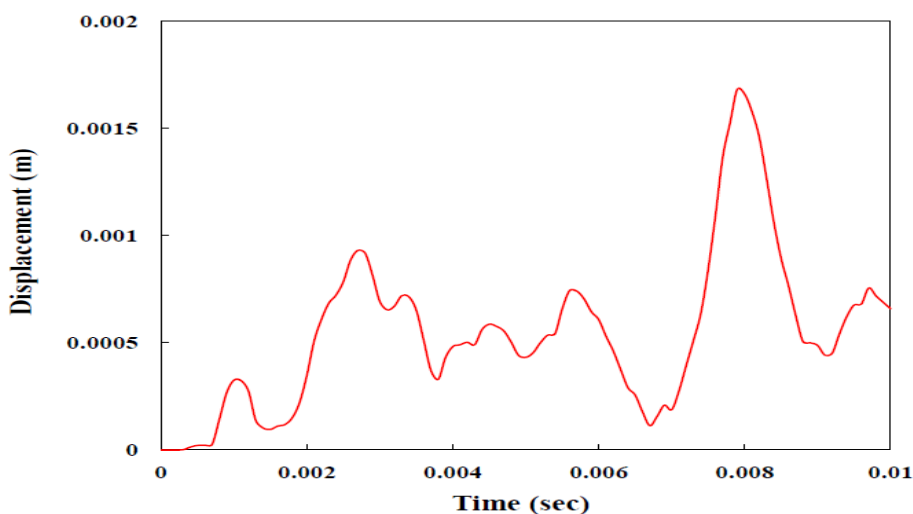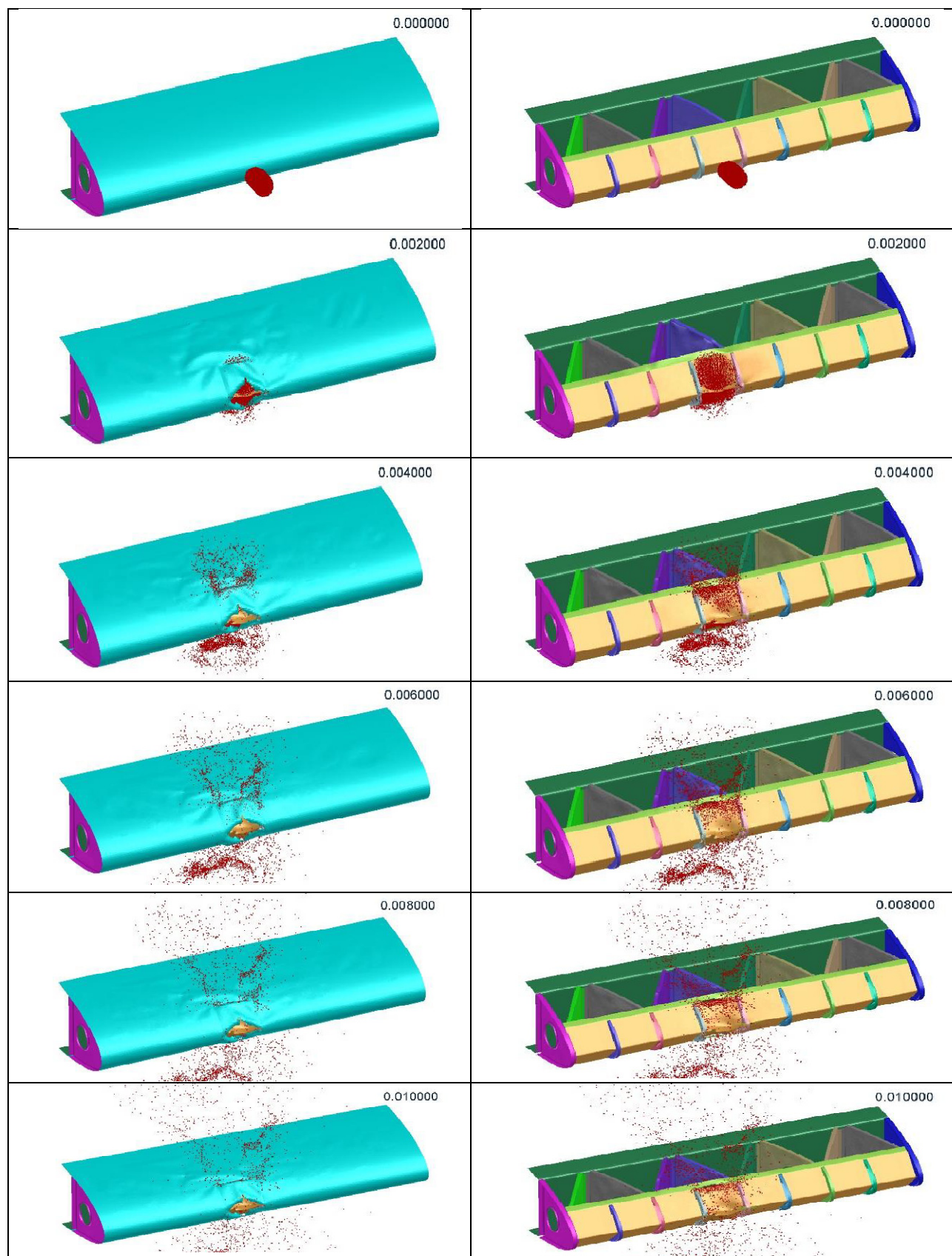
Figure-18: Case 2: Stress history for front spar.

Figure-19: Case 2: Displacement history for front spar.

Figure-20: Case 3: Condition of front ribs after bird impact.

Figure-21: Case 3: Wing leading edge condition with a time interval of 2ms.

Figure-22: Case-3: Stress history for front bar.

Figure-23: Case3: Displacement history for front bar.

Case 4: Leading Edge with a Wedge Support and Straight Front Ribs: In case 4, results show that bird impacts leading edge and penetrates skin. Then it hits the wedge support. Wedge support performs a cutting like action to the bird and splitting it into two pieces. Then these two pieces are cleared through top and bottom side of wing without hitting or penetrating the remaining structure. The striking bird penetrates the skin two times. First, when bird hits leading edge. Second time, when bird is deflected by wedge support in up and down. The bird penetrates though skin again and leaves wing leading edge. The condition of wing leading edge components for case 4 is shown in Figure-24.

In impact process, bird kinetic energy is reduced to 3.9 KJ from an initial value of 20.3 KJ. Wedge support absorbs an amount of 2.5 KJ of impact energy. Skin takes 3.6 KJ of impact energy. Like previous case, two front ribs on the sides of impact zone are almost destroyed and each takes about 0.34 KJ and 0.43 KJ of impact energy. Sub spar absorbs 0.85 KJ of energy while front spar takes only 0.07 KJ of energy. Rear ribs absorb more energy than case 2 and case 3. This value ranges from 0.2 KJ for rear right behind impact line to 0.01 KJ for rear rib present near side rib. The two side ribs absorb an amount of 0.02 KJ and 0.01 KJ of energy.

Although energy absorbed by front spar is higher than previous two cases but there is no plastic strain found in front spar. The maximum stress in front spar is found to be 236 MPa at time 2.8ms after impact. This maximum stress is found in area at lower left area mating with side rib. Maximum displacement is found to be 1.7 mm at middle of area mating with left side rib. Time history of stress and displacement for front spar is shown in Figure-25 and Figure-26 respectively.

Figure-24: Case 4: Wing leading edge condition with a time interval of 2ms.
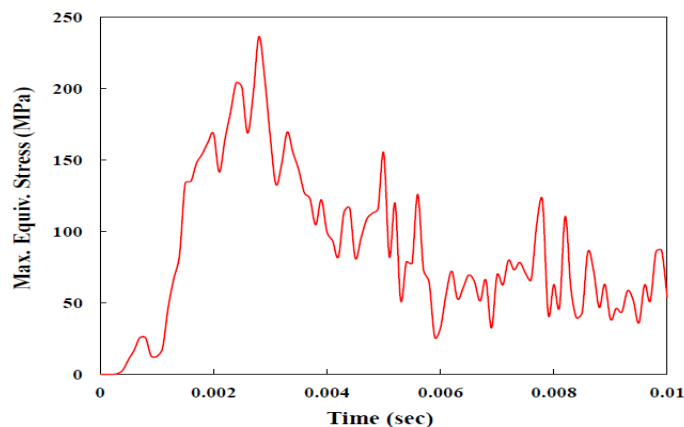
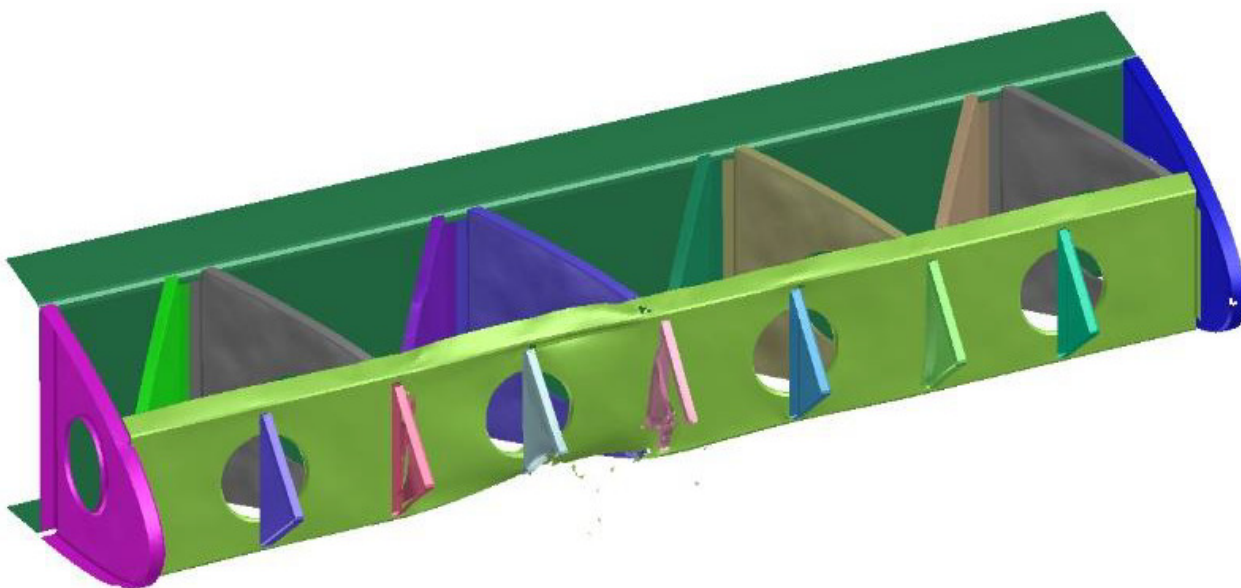**Figure-25:** Case 4: Stress history for front spar.
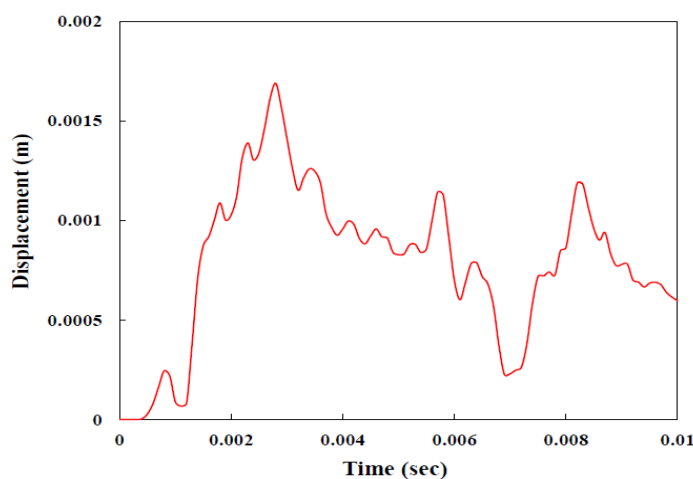
Figure-26: Case4: Displacement history for front spar.

Case 5: Leading Edge with a Wedge Support Having Inside Front Ribs: In this case, bird penetrates through skin after impact and then gets deflected by wedge support. Wedge support perform cutting action to the bird and splits it into two pieces which are deflected to the top and bottom of wedge support. However, some portion of the bird which is deflected downward penetrates through sub spar because of deflected wedge support.

This portion of bird is accumulated in area bounded by rear ribs, sub spar and front spar. Since leading portion of skin is not supported by any rib other than side ribs, skin waves and huge displacement and dent can be seen. Two front ribs, present near impact zone, are almost destroyed during bird impact process as shown in Figure-27. Step by step bird impact scenario with an interval of 2ms is shown in Figure-28.

Bird loses its kinetic energy to 3.2 KJ from an initial value of 20.3 KJ. Skin absorbs about 4.3 KJ of impact energy and internal energy of wedge support is increased to 2.5 KJ. The two destroyed ribs collectively absorb 0.64 KJ of energy. Sub spar takes about 1 KJ of energy while two rear ribs near impact line absorb 0.25 KJ and 0.21 KJ of energy.

Although front spar is hit with some part of deflected bird but no plastic strain is produced in spar. Maximum stress observed is 265 MPa and maximum displacement is 3 mm. time history of stress and displacement is shown in Figure-29 and Figure-30.

Figure-27: Case 5: Condition of front ribs after bird impact.
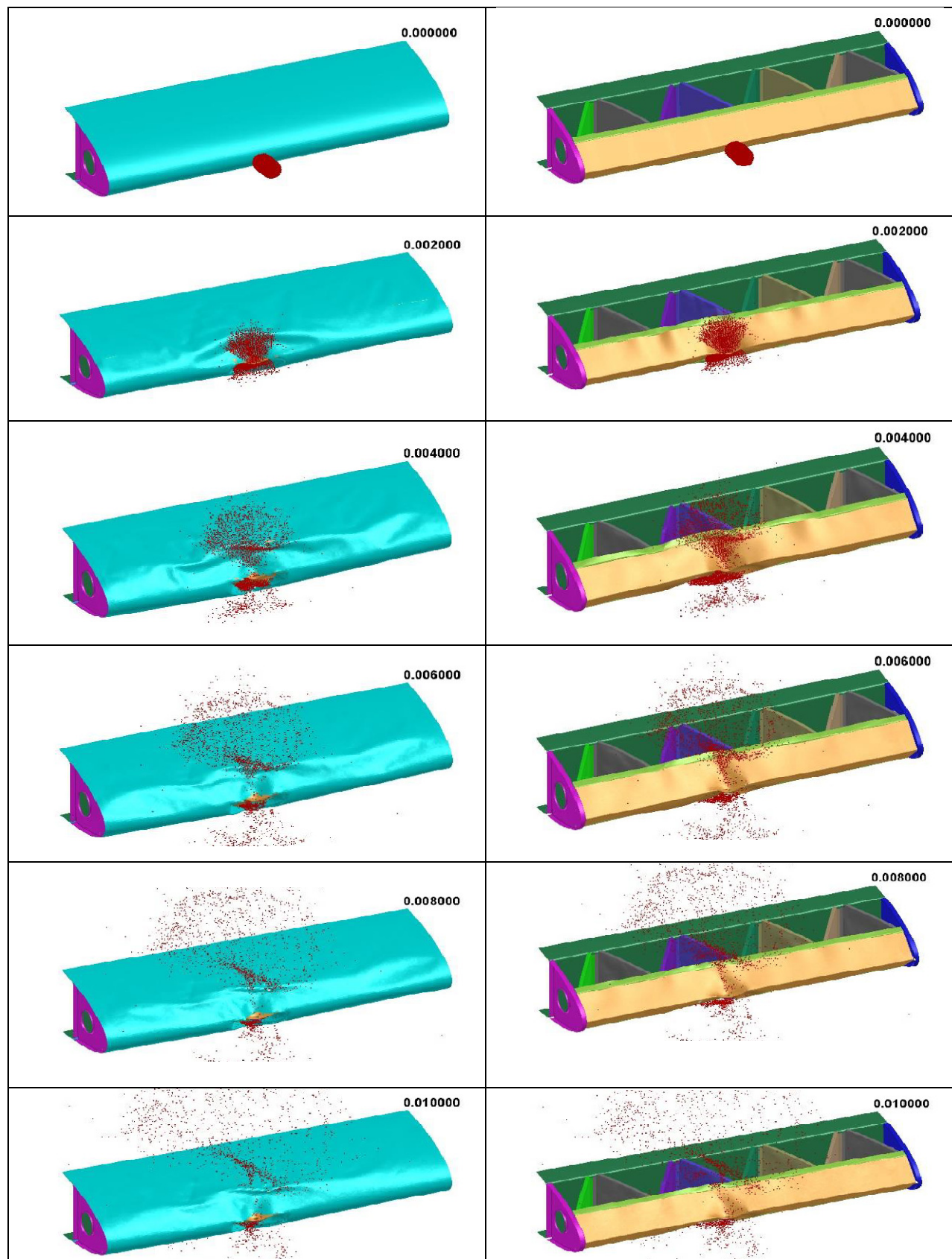
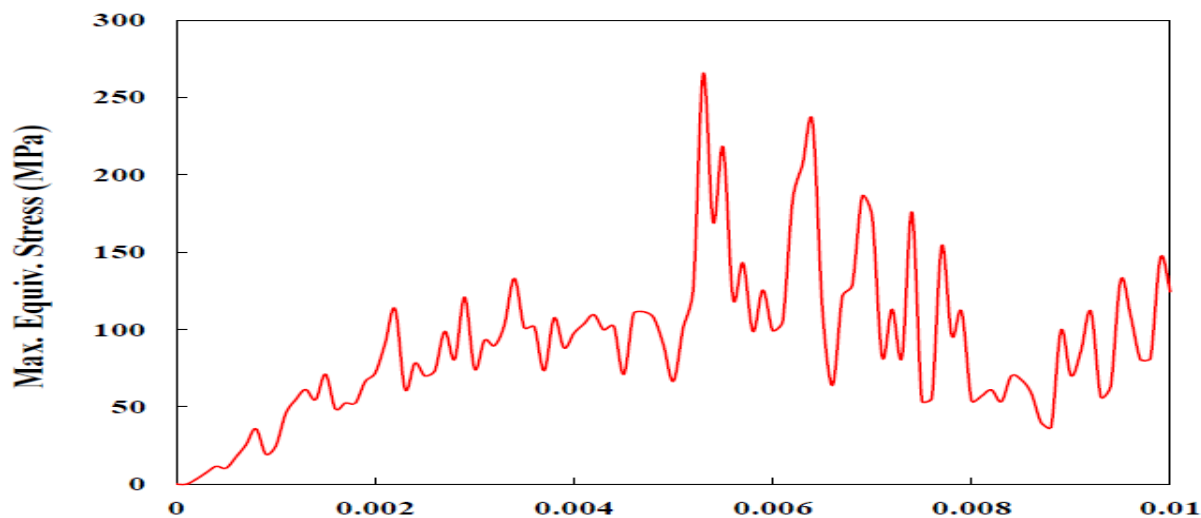**Figure-28:** Case 5: Wing leading edge condition with a time interval of 2ms.

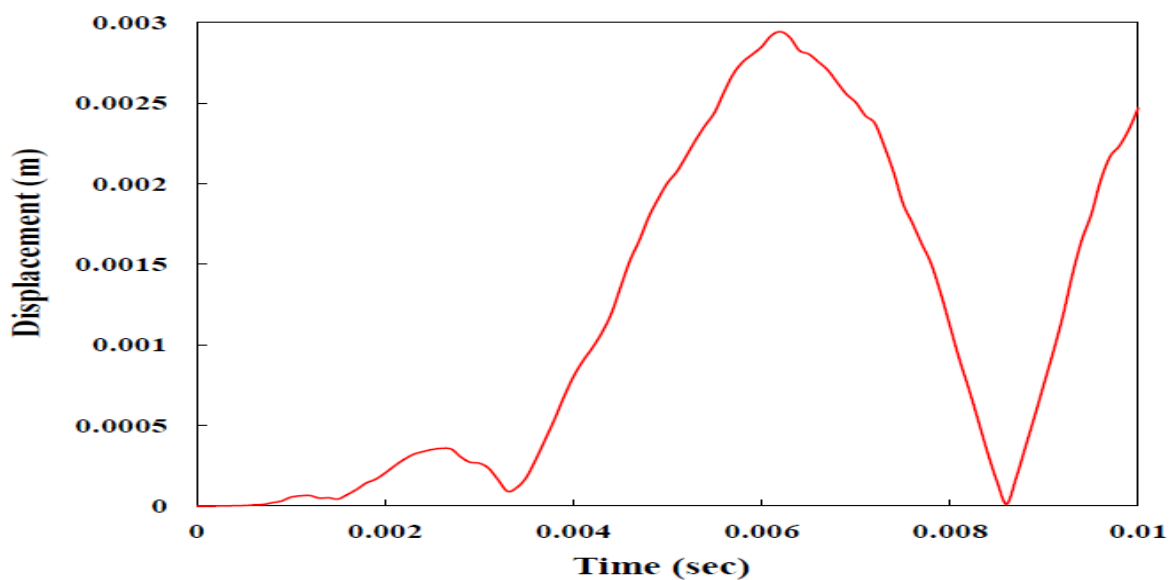**Figure-29:** Case5: Stress history for front spar.

Figure-30: Case5: Displacement history for front spar.

Case 6: Leading Edge with a Wedge Support having Angular Front Ribs: Like case 4, bird impacts the leading edge and penetrates the skin. Then it hits the wedge support and splits into two pieces travelling in upward and downward direction and escapes the leading-edge area. Angular front ribs in line of impact tries to compress the flowing bird along the wedge support. Meanwhile wedge support gets deflected on lower side and some of bird portion penetrates through sub spar and flows along skin and then hits the front spar. When bird travels half of the way along wedge support, front edge of wedge support, situated in impact area between front ribs, gets opened. Edges of front ribs to the end of wedge support get destroyed. Bird impact scenario for case 6 is shown in Figure-31 with a time step of 2ms. At the end of simulation, the bird is left with a kinetic energy of 3.25 KJ. Most of the impact energy is absorbed by skin like all other cases. It is about 3.1 KJ. Wedge support takes 2.9 KJ of impact energy. Two front ribs on either side of bird impact line absorb 0.69 KJ and 0.66 KJ of energy. As some portion of sub spar is hit by some part of bird, so energy absorbed by it is 1.1 KJ higher than previous all cases. The two rear ribs present in line of bird impact also absorb 0.3 KJ and 0.33 KJ of energy. Internal energy of front spar is increased by 0.06 KJ.

No plastic strain is produced in front spar during bird impact process. So, material behavior of front spar remains in elastic range. Maximum stress is found to be 283 MPa which is produced in lower area of front spar near skin, in the line of bird impact. Maximum displacement produced is 1.53 mm at the center of area between two rear ribs near to right side rib. Time history of stress and displacement is shown in Figure-32 and Figure-33.
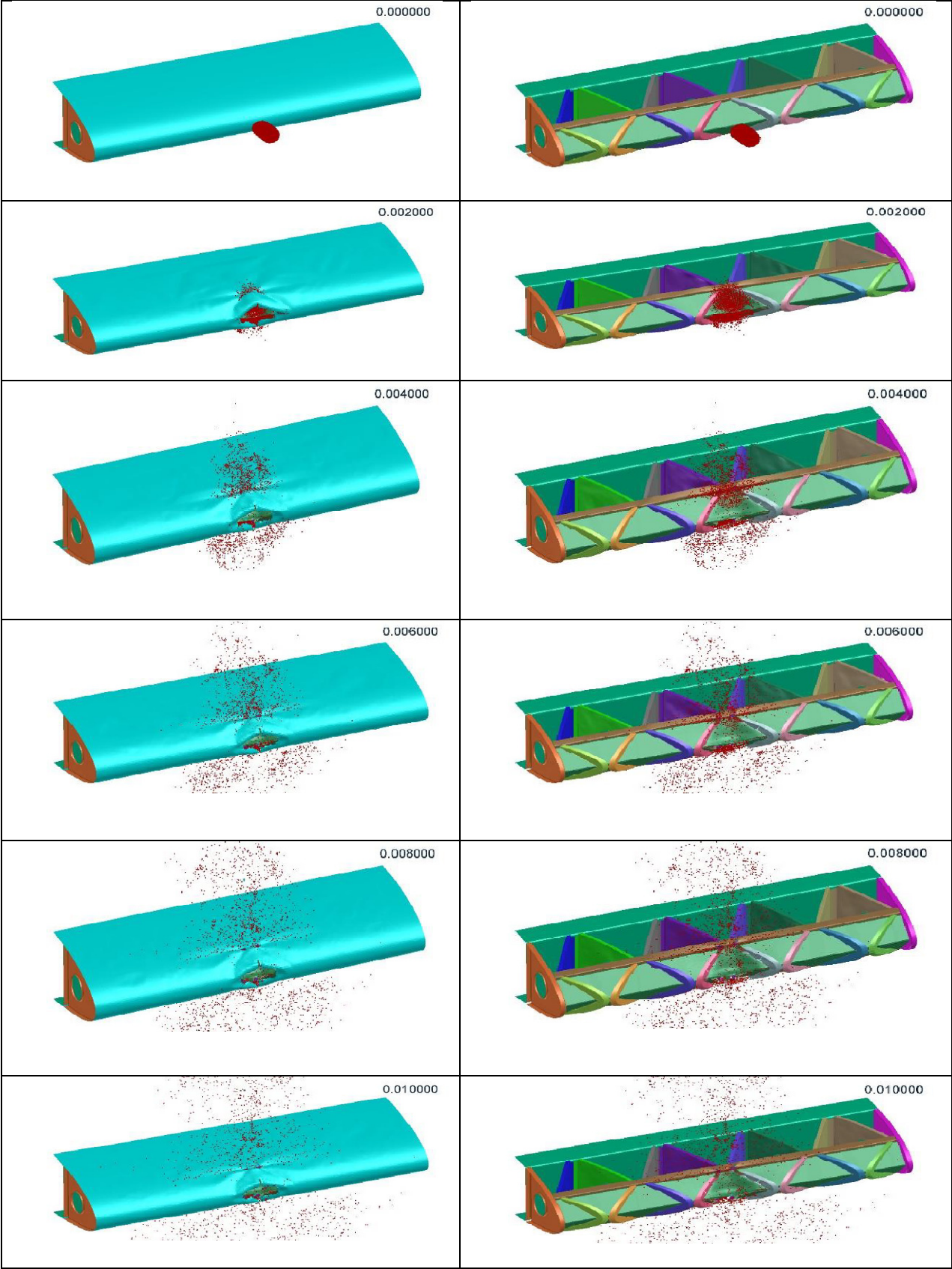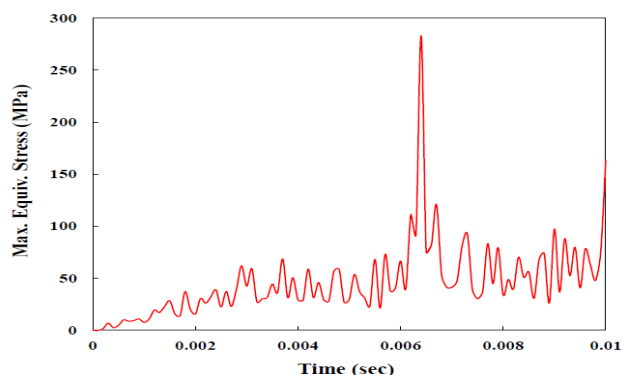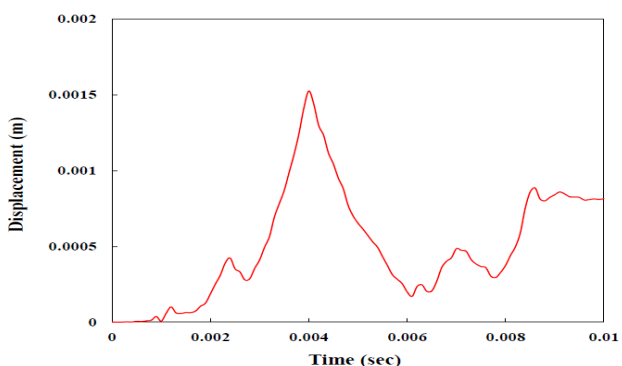
Figure-31: Case 6: Wing leading edge condition with a time interval of 2ms.

Figure-32: Case6: Stress history for front spar.

Figure-33: Case 6: Displacement history for front spar.

## Bird Strike Analysis: Second Scenario

It is noted for second scenario in all cases that when bird hits the leading edge, it creates a dent or cavity on skin and then slips away. A small portion of bird manages to penetrate the skin, bypasses the front structure before sub spar due to initial height and hits the front spar directly. In case 5, bird produces a long cut along its impact line which seems more prominent to other cases. Front spar stress level for case 1 is decreased while increased for all other cases. All other case other than case 1 also suffers from plastic strain. However, amount of these plastic strains is lesser from those which cases 1 suffers for scenario 1. The values of stress, strain and displacement produced in front spar for all cases in second scenario are listed in Table-4.

Table-4: Results for second scenario (Front spar only).

Case No.	Stress (MPa)	Plastic Strain	Displacement (mm)
1	375	0.0001	5.2
2	383	0.003	6
3	405	0.006	6.8
4	400	0.003	7
5	427	0.012	9.2
6	443	0.03	20

Time history of all the cases in second scenario are shown from Figure-34 to Figure-39 with a time step of 2ms.
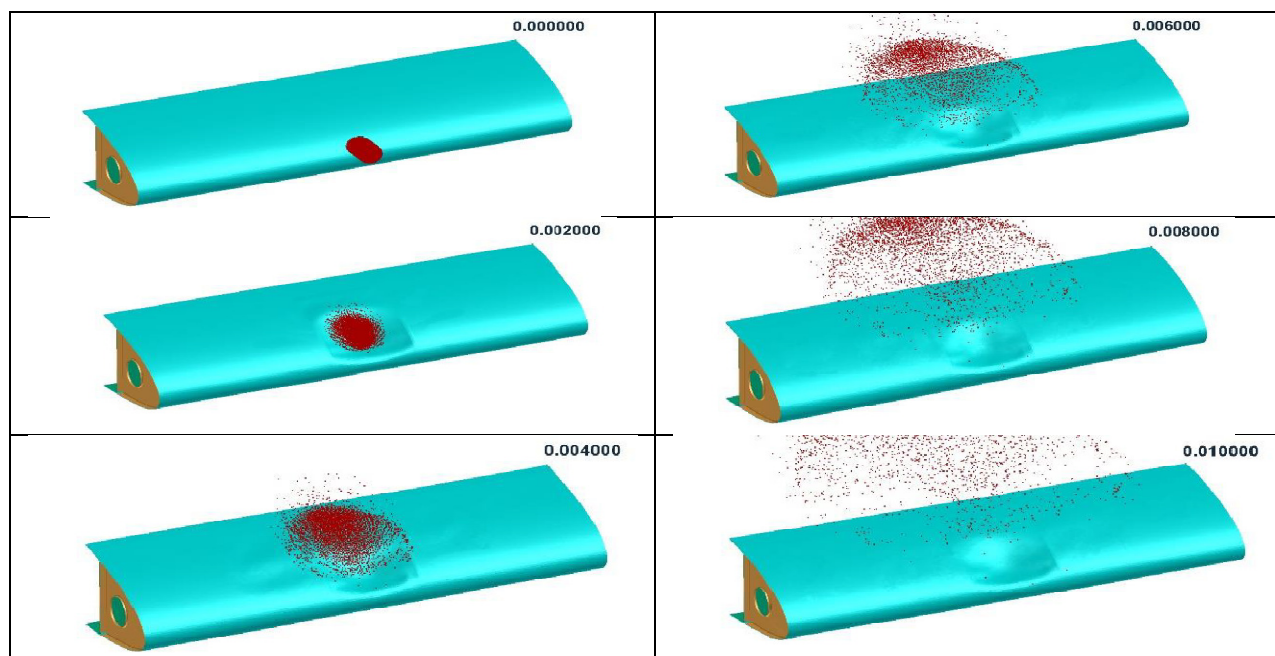
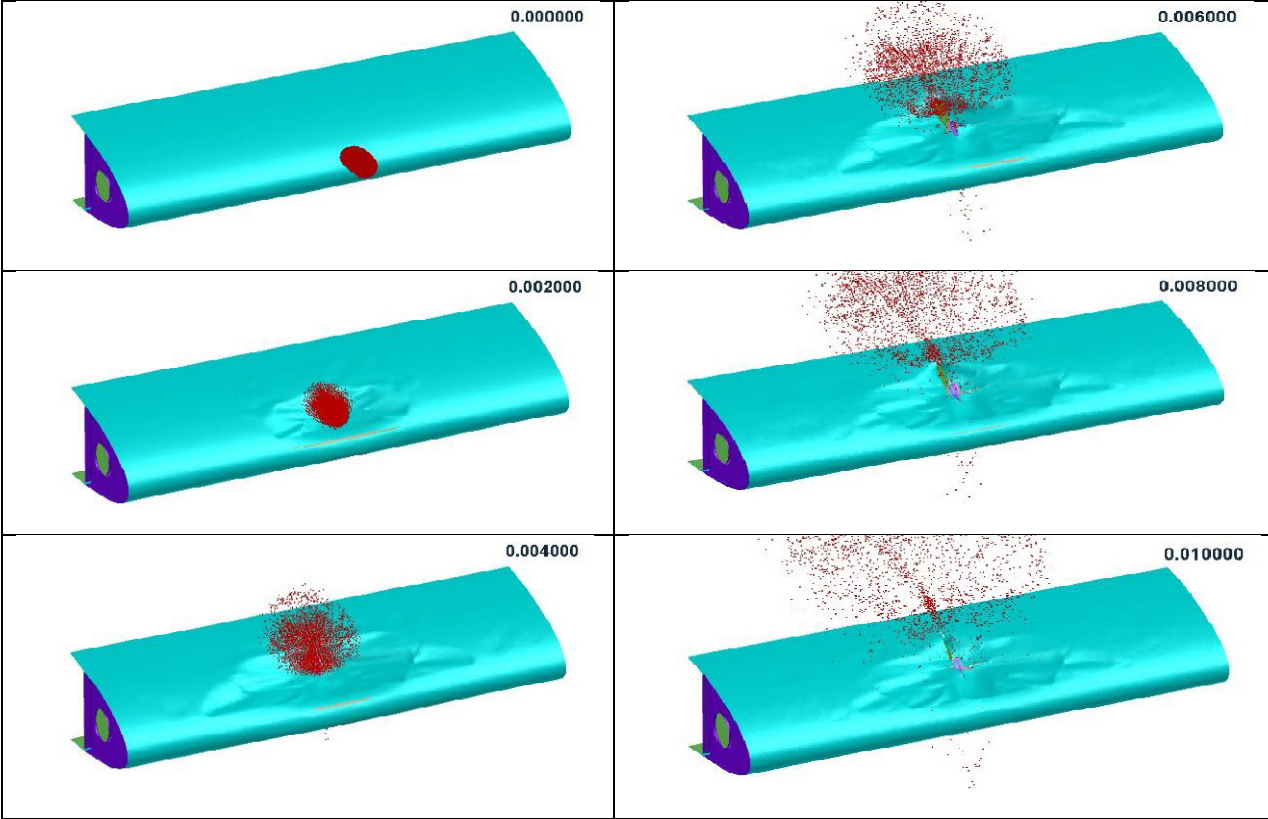**Figure-34:** Second Scenario Case 1: Wing leading edge condition.

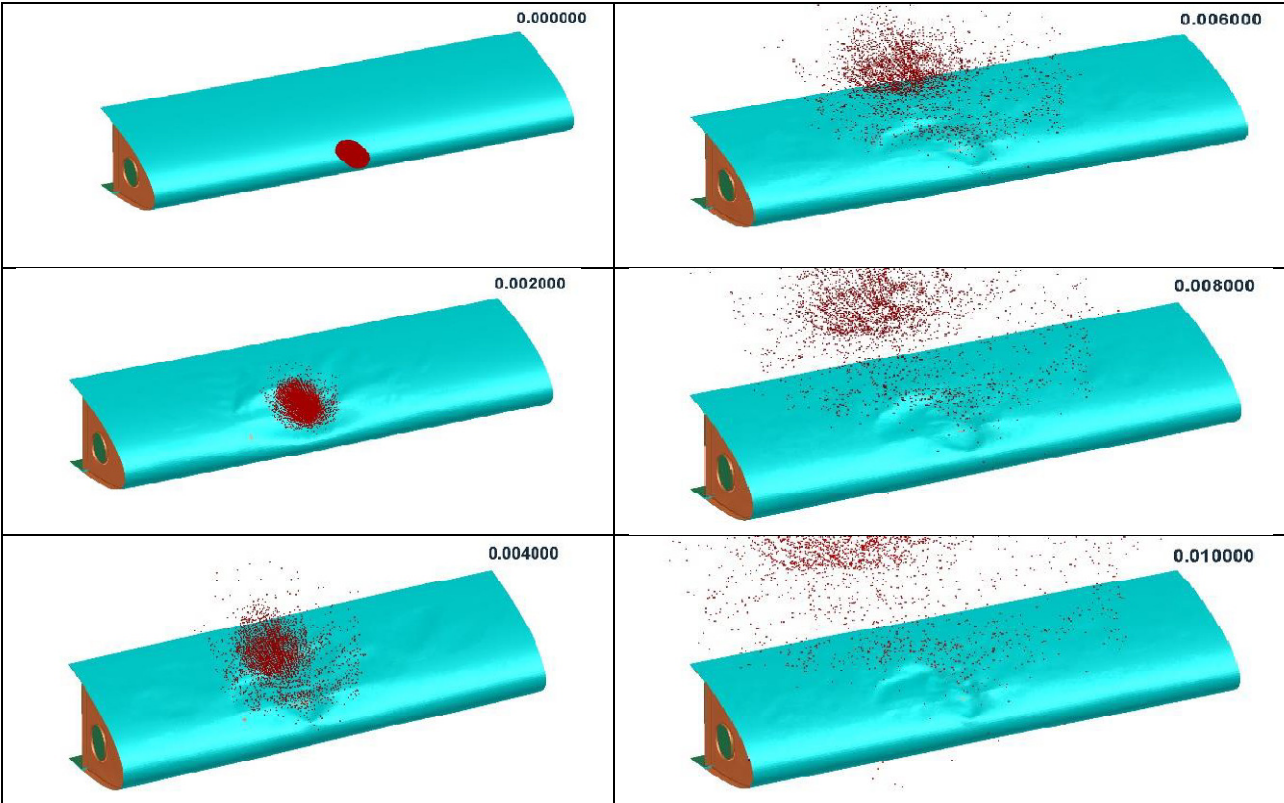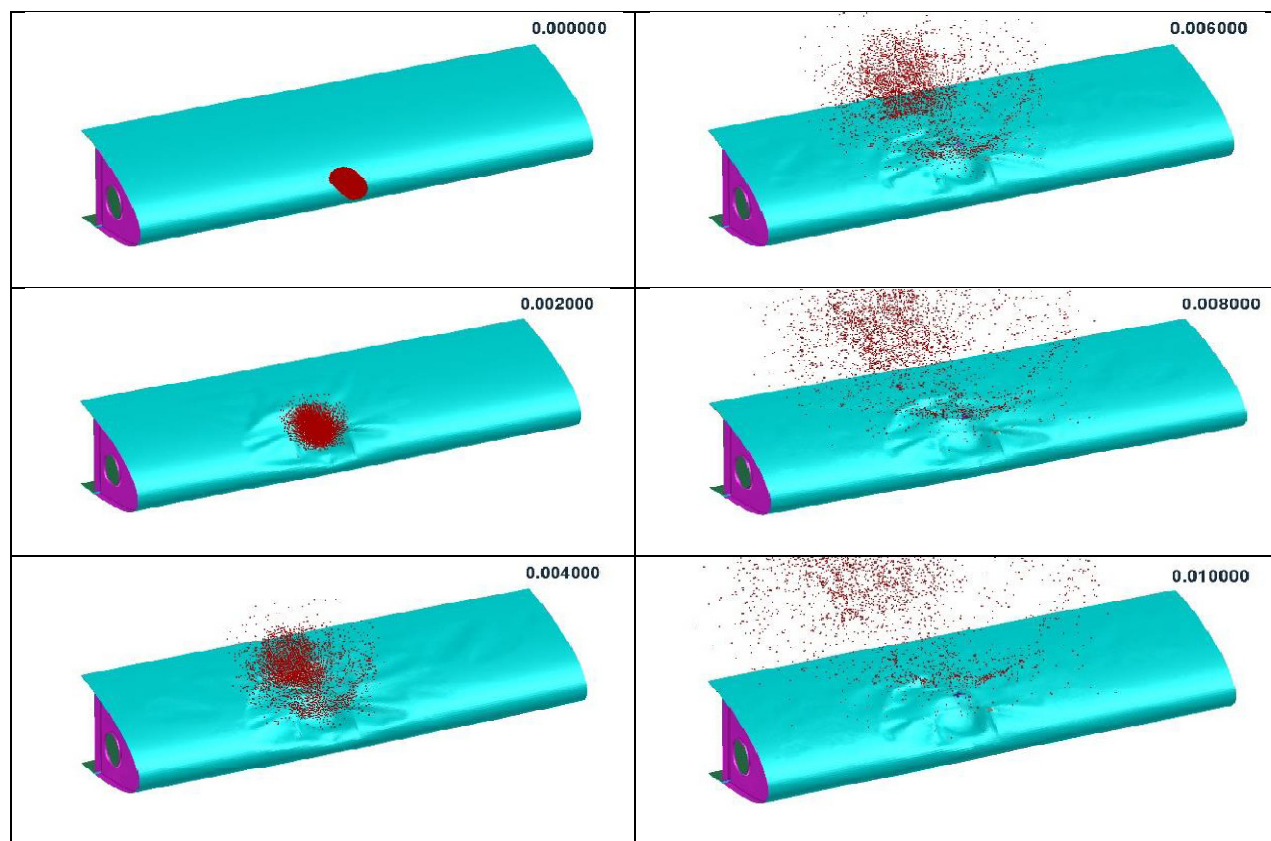**Figure-35:** Second Scenario Case 2: Wing leading edge condition.
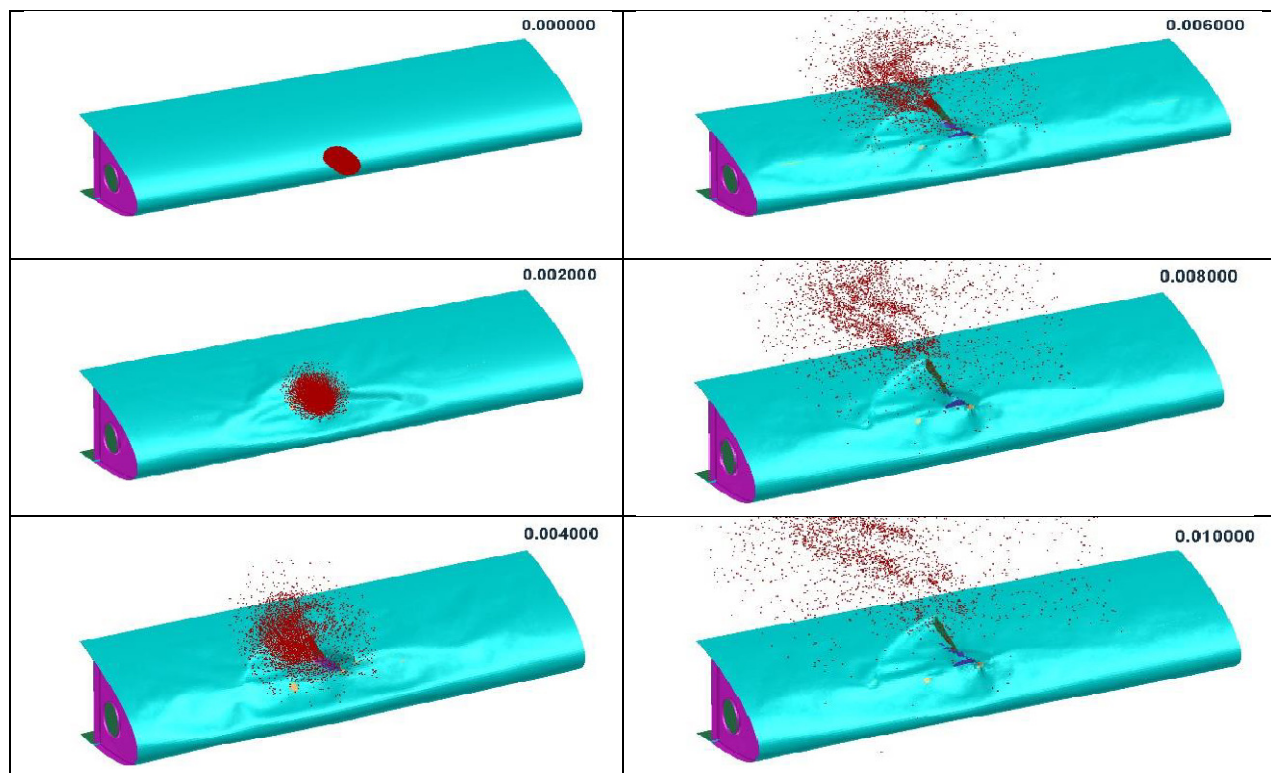

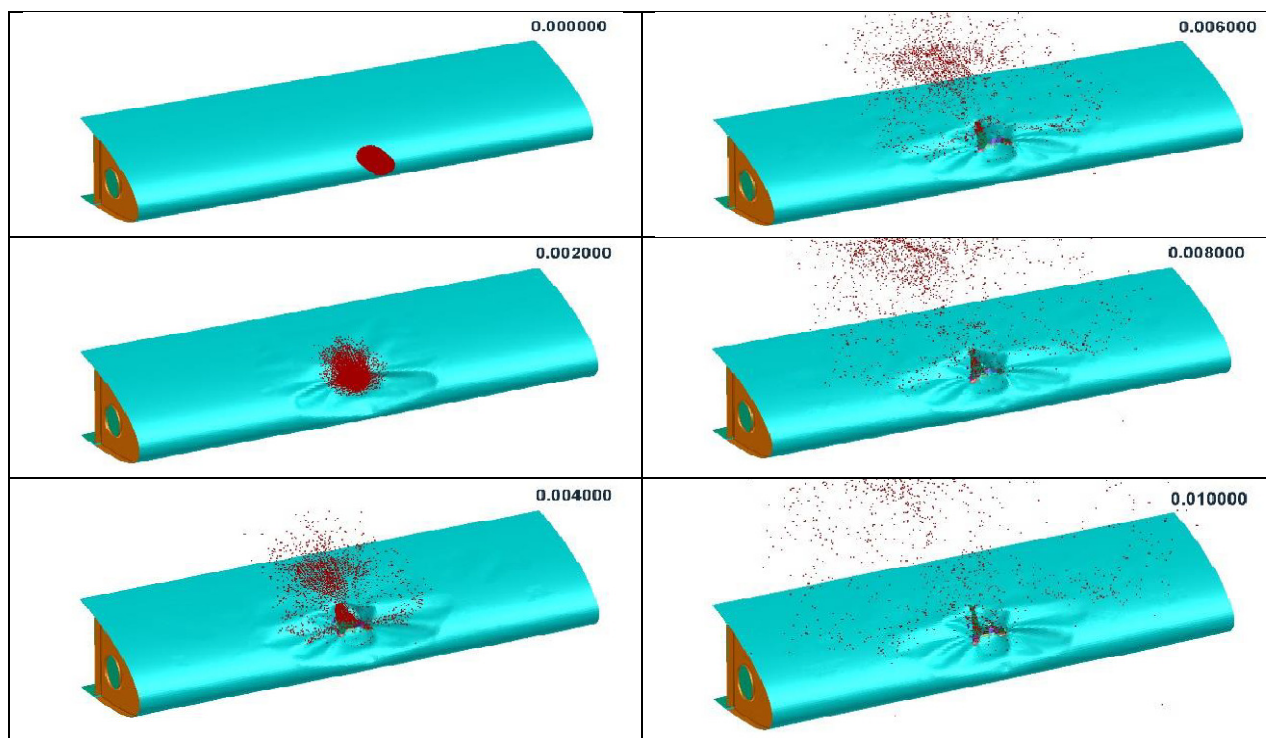**Figure-36:** Second Scenario Case 3: Wing leading edge condition.

Figure-37: Second Scenario Case 4: Wing leading edge condition.

Figure-38: Second Scenario Case 5: Wing leading edge condition.

Figure-39: Second Scenario Case 6: Wing leading edge condition.

Results Comparison

Bird Kinetic Energy Reduction: Figure-40 and Figure-41 show the process of bird losing its kinetic energy during its impact. In first scenario, bird loses maximum energy for case 1 and minimum for case 3. For other four cases, bird loses its energy almost in same pattern. In second scenario, bird loses its maximum energy for case 6 and minimum for case 1. Energy losing pattern of bird is same for all cases except case 6 which follows a slightly different path. In second scenario cases, energy lost by bird is lesser than cases of first scenario.

Maximum Stress: Stress level in front spar for both scenario cases is shown in Figure-42. Except case 1, maximum stress in front spar for first scenario is lesser than second scenario. In first scenario, stress is maximum for case 1 and minimum for case 3. In second scenario, stress is maximum for case 6 and minimum for case 1.

Maximum Plastic Strain: In first scenario, no of case other than case 1 experiences plastic strain. Plastic strain value for case 1 in first scenario is the highest for both scenarios and all cases. In second scenario, plastic strain is produced in all the cases. This value is much smaller for case 1. Comparison of plastic strain for both scenarios is shown in Figure-43.

Maximum Displacement: Displacement values follow the same pattern like plastic strains as shown in Figure-44. Displacement produced in case 1 for first scenario is the largest value. Other cases in first scenario experiences almost same

displacement. In second scenario, displacement for case 6 is higher than others. Other cases in second scenario experience almost same value of displacement.
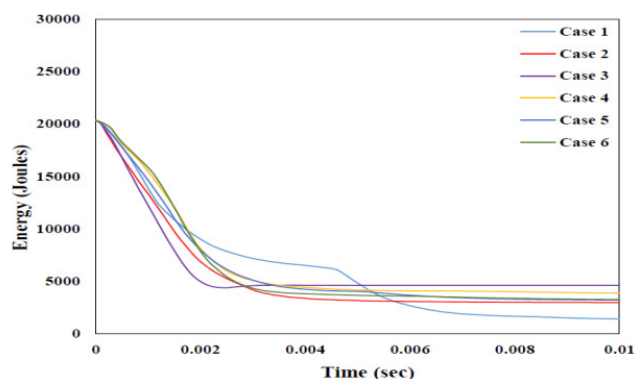
Figure-40: K.E. lost by bird in 1st scenario.
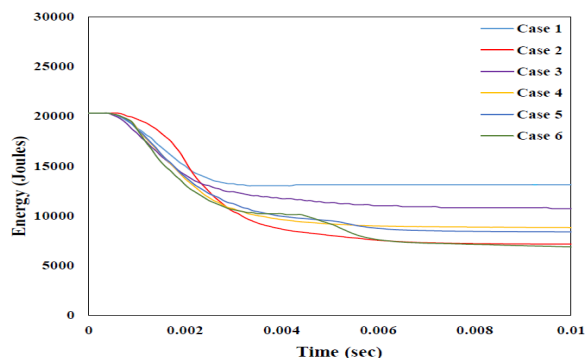
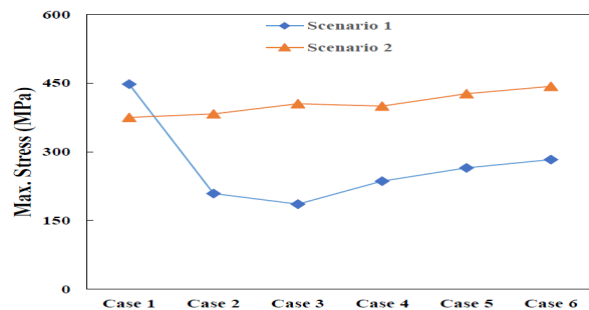**Figure-41**: K. E. lost by bird in 2nd scenario.

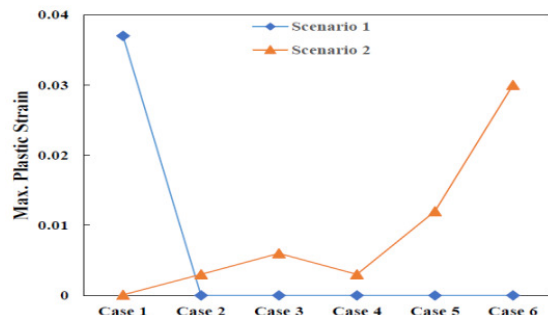**Figure-42:** Max. stress (Front spar only).

Figure-43: Max. plastic strain (Front spar only).

Structural Weight: Since structural weight is the major constraint in design of different cases, therefore weight for all cases measure close to one another. Case 1 is the heaviest and case 3 is the lightest. Weight comparison of all cases is shown in Figure-45.
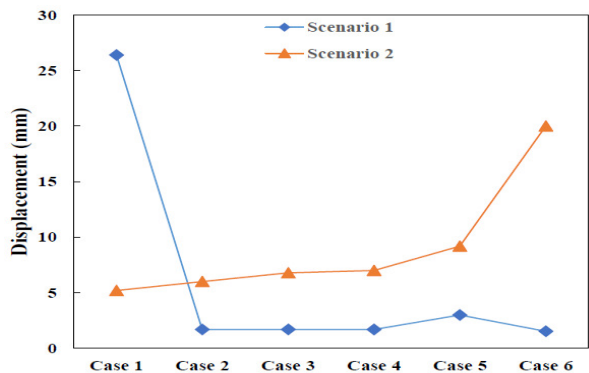

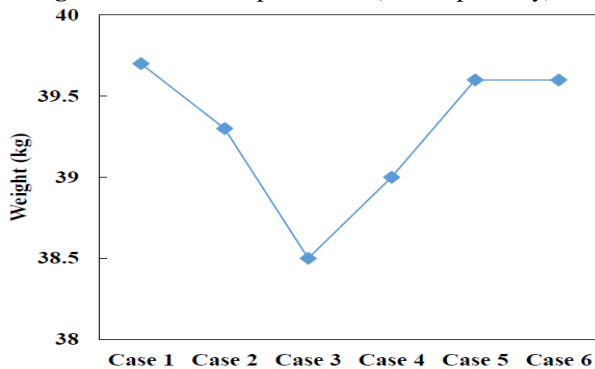**Figure-44:** Max. Displacement (Front spar only).

Figure-45: Structural weight comparison.

Conclusion

In this research, it is tried to provide a new design of wing leading structure which can resist to bird strike more efficiently, without adding extra weight to aircraft. Five new design has been studied against traditional design. Those have been analyzed using FEM tools and data available in literature. Each design is tested against same bird weight, shape and speed. Two scenarios of bird strike are considered for analysis. Main emphasis of all new designs centers the safety of front spar of wing.

Traditional wing leading edge (case 1) has lesser parts but parts are thicker. When case 1 is tested against bird strike for first scenario, front spar suffers with a large amount of plastic strain which is the largest value for all cases.

Then case 1 is analyzed for second scenario. Case 1 is proved well in this scenario and suffers much lower stress and strain to first scenario. Behavior of case 1 in second scenario is also found the best to all other cases.

Case 2 has more components than case 1 but its weight is lower than case 1 by using thin components. This case does not allow the penetration of bird through skin for first scenario. The behavior of front spar remains in elastic range as there is no plastic strain produced in the spar and stress is also well below yield strength. When case 2 is tested for second scenario, it allows little amount of bird penetration due to which some amount of plastic strain is produced in front spar.

Case 3 also does not permit bird penetration for first scenario. Behavior of front spar is well in elastic range and stress is well below yield strength. Deflection produced in spar is also very small. For second scenario, this case suffers a little amount of plastic strain as a small part is escaped through skin and hits the front spar. The weight of leading edge is found to be lightest of all designs.

Case 4, by design, permits bird penetration though skin allowing it to hit on wedge support. Thus, bird is splitted into two pieces, cleared through top and bottom of wing leading edge without penetrating through remaining structure. Front spar suffers low stress for first scenario and its mechanical behavior remains in elastic limit. However, spar is exposed to some value of plastic strain in second scenario.

In case 5, front spar experiences low stress and less deflection for first scenario but skin is dented and damaged heavily due to absence of support to skin in frontal area. Analyzed in second scenario, skin is sheared along the bird flow path producing plastic strain in front spar and causing high stress.

Case 6 is also behaving well for first scenario and does not show plastic behavior due to low value of stress. When put against second scenario, this design suffers the largest value of plastic strain.

Keeping the weight constraint in front and considering safety of front spar, it can be concluded that case 2, 3 and 4 are better designs for wing leading edge structure. These designs almost behave similarly for front spar safety.

Future Work: In future, weight optimization of these designs can be performed. These designs are vulnerable to second scenario to a small extent. So, designs can be modified to show good results in both scenarios. These designs can be manufactured and tested practically to confirm the results of analysis. As composites are widely being used in aviation industry, so new designs for wing leading edge resistive to bird strike based on composite materials can also be put to research.

Acknowledgement

References

1. MacCinnon B. (2004). Sharing the Skies: An Aviation Industry Guide to the Management of Wildlife Hazards. Report TP.

2. Dolbeer S.E.W.R.A. and Weller John R. (July 2014). Wildlife strikes to civil aircraft in the United States 1990-2013. Federal Aviation Administration.

3. Katukam R. (2014). Compreshensive Bird Strike Simulation Approach for Aircraft Structure Certification. CYIENT.

4. Liu J., Li Y., Gao X. and Yu X. (2014). A numerical model for bird strike on sidewall structure of an aircraft nose. *Chinese Journal of Aeronautics*, 27(3), 542-549.

5. Grimaldi A., Sollo A., Guida M. and Marulo F. (2013). Parametric study of a SPH high velocity impact analysis – A birdstrike windshield application. *Composite Structures*, 96, 616-630.

6. Y. Guo, P. Jia and G. Hong (2012). Research on Bird Strike Simulation of Composite Leading Edge. *AASRI Procedia*, 3, 674-679.

7. Smojver I. and Ivancevic D. (2010). Bird impact at aircraft structure–Damage analysis using Coupled Euler Lagrangian Approach. IOP Conference Series: Materials Science and Engineering, 10(1), 012050.

8. Dar U.A., Zhang W. and Xu Y. (2013). FE Analysis of Dynamic Response of Aircraft Windshield against Bird Impact. *International Journal of Aerospace Engineering*, 1-12.

9. N.R.V. Nikhil K.V (2014). Impact Analysis of Soft Ellipsoidal Projectile with Void on Rigid Wall. *International Journal of Research in Aeronautical and Mechanical Engineering*, 2(3), 165-174.

10. Salem S.C., Viswamurthy S.R. and Sundaram R. (2011). Prediction of Bird Impact behavior through Different bird models using Altair Radioss. HTC, 1-9.

11. Goyal V.K., Huertas C.A. and Vasko T.J. (2014). Smooth Particle Hydrodynamics for Bird-Strike Analysis Using LS-DYNA. *American Transactions on Engineering & Applied Sciences*, 2(2), 83-107.

12. Velmurugan V.N. (2017). Numerical bird strike impact simulation of aircraft composite structure. IOSR *Journal of Mechanical and Civil Engineering* (IOSR-JMCE), 2, 1-10.

13. Ugrcic M., Maksimovic S., Stamenkovic D., Maksimovic K. and Nabil K. (2015). Finite element modeling of wing bird strike. FME Transaction, 43(1), 76-81.

14. Xue P., Zhao N., Liu J. and Li Y.L. (2011). Approach to Assess Bird Strike Resistance for a Wing Slat Structure. *Journal of Aircraft*, 48(3), 1095-1098.

15. Reglero J.A., Rodríguez-Pérez M.A., Solórzano E. and Saja de J.A. (2011). Aluminium foams as a filler for leading edges: Improvements in the mechanical behaviour under bird strike impact tests. *Materials & Design*, 32(2), 907-910.

16. Sun Y.J.L.R.H.J.Q. (2014). Numerical simulation of bird strike in aircraft leading edge structure using a new dynamic failure model. in 29th Congress of International Council of the Aeronautical Sciences, st. Petersburg.

17. Doubrava R. and Strnad V. (2010). Bird Strike Analyses on The Parts of Aircraft Structure. in 27th International Congress of The Aeronautical Sciences, Nice, France.

18. Hedayati R. and Ziaei-Rad S. (2013). A new bird model and the effect of bird geometry in impacts from various orientations. *Aerospace Science and Technology*, 28(1), 9-20.

19. KavithaMol S., Stanley and Salem S.C. (2011). Target parametric studies on bird impact behaviour of aircraft leading edges. National Aerospace Laboratories, Bangalore.

20. Liu J., Li Y., Shi X. and Wang W. (2012). Dynamic Response of Bird Strike on Aluminum Honeycomb-Based Sandwich Panels. *Journal of Aerospace Engineering*, 27(3), 520-528.

21. Heimbs S. (2011). Computational methods for bird strike simulations: A review. Computers & Structures, 89(23), 2093-2112.

22. Airoldi A. and Cacchione B. (2006). Modelling of impact forces and pressures in Lagrangian bird strike analyses. *International Journal of Impact Engineering*, 32(10), 1651-1677.

23. Lavoie M.A., Gakwaya A., Ensan M.N., Zimcik D.G. and Nandlall D. (2009). Bird's substitute tests results and evaluation of available numerical methods. *International Journal of Impact Engineering*, 36(10), 1276-1287.

24. Nizampatnam L.S. (2007). Models and methods for bird strike load predictions. Wichita State University.

25. Johnson A.F. and Holzapfel M. (2003). Modelling soft body impact on composite structures. *Composite Structures*, 61(1), 103-113.

26. McCarthy M.A., McCarthy C.T., Kamoulakos A., Ramos J., Gallard J.P. and Melito V. (2004). Modelling of bird strike on an aircraft wing leading edge made from fibre metal laminates - Part 2: Modelling of impact with SPH bird model. *Applied Composite Materials*, 11(5), 317-340.

27. Yupu G., Zhenhua Z., Wei C. and Deping G. (2008). Foreign Object Damage to Fan Rotor Blades of Aeroengine Part II: Numerical Simulation of Bird Impact. *Chinese Journal of Aeronautics*, 21(4), 328-334.

28. McCarthy M.A., Xiao J.R., McCarthy C.T., Kamoulakos A., Ramos J., Gallard J.P. and Melito V. (2005). Modelling bird impacts on an aircraft wing – Part 2: Modelling the impact with an SPH bird model. I*nternational Journal of Crashworthiness*, 10(1), 51-59.